ing the size of the pore structure in the sponge. Therefore, because the PGA(+) sponge can accept and keep a sufficient volume of the cell mixture, the grafted cells can be retained within the sponge. Perhaps because of this, little ectopic hair formation was observed in the grafted sites of the PGA(+) sponge. Furthermore, the movement of the transferred cells did not seem to be inhibited in the PGA(+) sponge, and as a result this may have suppressed the formation of epidermal cysts. Thus, it is likely that not only the cellular requirements but also the cell positions and movements are important for proper restructuring of hair follicles, inferring from the process of hair morphogenesis that the epithelium grows downward into the dermis as a plug that joins at its proximal end a mesenchymal condensation, referred to as the dermal papilla.[1,2]

Moreover, because the incorporation of PGA fibers confers to the collagen sponge the ability to resist mechanical deformation, the PGA(+) sponge has the ability to be transformed into various shapes, raising the possibility that it could be embedded as a scaffold even on an irregular graft bed. Future advances in the cell biological study of hair formation may, using the PGA(+) collagen sponge, allow for three-dimensional skin reconstitution cultures with skin appendages and subsequent cell transplantation therapy into patients.

ACKNOWLEDGMENTS

The authors thank Dr. Steven D. Emmet for advice on preparing the manuscript in English. This work was supported by a health science research grant from the Japanese Ministry of Health, Labor, and Welfare.

REFERENCES

1. Stenn, K.S., and Paus, R. Controls of hair follicle cycling. Physiol. Rev. **81,** 449, 2001.
2. Millar, S.E. Molecular mechanisms regulating hair follicle development. J. Invest. Dermatol. **118,** 216, 2002.
3. Alonso, L., and Fuch, E. Stem cell in the skin: Waste not, Wnt not. Genes Dev. **17,** 1189, 2003.
4. Worst, P.K.M., Mackenzie, I.C., and Fusenig, N.E. Reformation of organized epidermal structure by transplantation of suspensions and cultures of epidermal and dermal cells. Cell Tissue Res. **225,** 65, 1982.
5. Kamimura, J., Lee, D., Baden, H.P., Brissette, J., and Dotto, G.P. Primary mouse keratinocyte cultures contain hair follicle progenitor cells with multiple differentiation potential. J. Invest. Dermatol. **109,** 534, 1997.
6. Lichti, U., Weinberg, W.C., Goodman, L., Ledbetter, S., Dooley, T., Morgan, D., and Yuspa, S.H. In vivo regulation of murine hair growth: Insights from grafting defined cell populations onto nude mice. J. Invest. Dermatol. **101,** 124s, 1993.
7. Weinberg, W.C., Goodman, L.V., George, C., Morgan, D.L., Ledbetter, S., Yuspa, S.H., and Lichti, U. Reconstitution of hair follicle development in vitro: Determination of follicle formation, hair growth, and hair quality by dermal cells. J. Invest. Dermatol. **100,** 229, 1993.
8. Kishimoto, J., Ehama, R., Wu, L., Jiang, S., Jiang, N., and Burgeson, R.E. Selective activation of the versican promoter by epithelial–mesenchymal interactions during hair follicle development. Proc. Natl. Acad. Sci. U.S.A. **96,** 7336, 1999.
9. Cotsarelis, G., Sun, T., and Lavker, R.M. Label-retaining cells reside in the bulge area of pilosebaceous unit: Implications for follicular stem cells, hair cycle, and skin carcinogenesis. Cell **61,** 1329, 1990.
10. Kobayashi, K., Rochat, A., and Barradon, Y. Segregation of keratinocyte colony-forming cells in the bulge of the rat vibrissa. Proc. Natl. Acad. Sci. U.S.A. **90,** 7391, 1993.
11. Rochat, A., Kobayashi, K., and Barrandon, Y. Location of stem cells of human hair follicles by clonal analysis. Cell **76,** 1063, 1994.
12. Oshima, H., Rochat, A., Kedzia, C., Kobayashi, K., and Barrandon, Y. Morphogenesis and renewal of hair follicles from adult multipotent stem cells. Cell **104,** 233, 2001.
13. Yuspa, S.H., Morgan, D.L., Walker, R.J., and Bates, R.R. The growth of fetal mouse skin in cell culture and transplantation to F_1 mice. J. Invest. Dermatol. **55,** 379, 1970.
14. Ueda, H., and Tabata, Y. Polyhydroxyalkanonate derivatives in current clinical applications and trials. Adv. Drug Deliv. Rev. **55,** 501, 2003.
15. Hiraoka, Y., Agr, M., Kimura, Y., Eng, M., Ueda, H., and Tabata, Y. Fabrication and biocompatibility of collagen sponge reinforced with poly(glycolic acid) fiber. Tissue Eng. **9,** 1101, 2003.
16. Yannas, I.V., and Burke, J.F. Design of an artificial skin. I. Basic design principles. J. Biomed. Mater. Res. **14,** 65, 1980.
17. Bell, E., Ehrlich, H.P., Buttle, D.J., and Nakatsuji, T. Living tissue formed in vitro and accepted as skin-equivalent tissue of full thickness. Science **211,** 1052, 1981.
18. Hansbrough, J.F., Boyce, S.T., Cooper, M.L., and Foreman, T.J. Burn wound closure with cultured autologous keratinocytes and fibroblasts attached to a collagen–glycosaminoglycan substrate. JAMA **262,** 2125, 1989.
19. Maruguchi, T., Maruguchi, Y., Suzuki, S., Matsuda, K., Toda, K., and Isshiki, N. A new skin equivalent: Keratinocytes proliferated and differentiated on collagen sponge containing fibroblasts. Plast. Reconst. Surg. **93,** 537, 1994.

Address reprint requests to:
Hitoshi Okochi, M.D., Ph.D.
Department of Tissue Regeneration
Research Institute, International Medical Center of Japan
1-21-1 Toyama, Shinjuku-ku, Tokyo 162-8655, Japan

E-mail: hokochi@ri.imcj.go.jp

表　題

著者名

醫學のあゆみ　別　刷

第　巻・第　号：　　年　月　日号

ウイルス性肝炎の現況と展望

別冊 医学のあゆみ

編集／熊田博光　虎の門病院消化器科

B5判・162頁・定価3,570円（本体3,400円 税5%）

●ウイルス性肝炎は現在，AからEまでが存在するが，肝炎の治療に対する考え方のほとんどはB型肝炎とC型肝炎が中心となっている．

●遺伝子学の発展によりB型肝炎の種々の遺伝子の要因および役割が明確となり，e抗原，e抗体に関する変化についても，Preコア領域の1896番目のコドンがTGGからTAGに変わることによりe抗原の産生が終息すると考えられたが，劇症肝炎においてはPreコア領域の変異，あるいはコアプロモーターの変異などが原因であることも明らかとなっている．したがって，いまなおB型肝炎に対する考え方も変わりつつある．

●B型慢性肝炎に対してわが国では，2000年11月より核酸アナグロであるラミブジンが発売になり広く使われているが，ラミブジンは長期投与がよいのか，あるいは短期投与がよいのか，その適用に関しての意見が分かれている．

●C型肝炎の治療に関しては，2001年リバビリン，コンセンサスインターフェロンの発売以降，インターフェロン領域の治療法が大きく変わってきた．

●本書では，ウイルス性肝炎の研究の進歩を基礎・臨床の両面から，現況と今後の発展性について紹介．

CONTENTS

医歯薬出版株式会社／〒113-8612 東京都文京区本駒込1-7-10／TEL.03-5395-7610 FAX.03-5395-7611

2004年1月作成 TP

皮膚科学

皮膚の多能性幹細胞

Multipotent stem cell in skin

皮膚の多能性幹細胞に関する研究は，21世紀の幕開けとともに2001年に大きな進展をみた．皮膚は表皮，真皮よりなるが，皮下の脂肪組織を含めて，この年だけで三者それぞれに多能性幹細胞が存在することが報告された．ES細胞(胚性幹細胞)や骨髄間葉系幹細胞と同様に，皮膚の細胞を幹細胞ソースとしてとらえられるようになった．

表皮の多能性幹細胞

もともと表皮は一生涯更新しつづける組織なので，幹細胞の存在は自明の理とされていた．毛包バルジ領域(立毛筋付着部位)に非常にゆっくり分裂する細胞の存在が示唆されていたが，2001年Oshimaらがバルジの移植実験により，バルジ領域の細胞が毛にも脂腺にも表皮にもなりうることを示した[1]．その後，一度表皮細胞に分化した細胞(ケラチン14陽性)をマウスの胚盤胞に注入すると，発生の過程で皮膚以外の細胞に分化しうることが示された[2]．また最近では，骨髄で最初に見出されたヘキスト33342という色素の排出能の高い細胞(side population cell：SP細胞)が表皮にも存在し，表皮由来のSP細胞を筋ジストロフィーのモデルマウスに静注したところ，筋細胞に分化することが報告された[3]．

以上の結果より，バルジ領域に多能性幹細胞が存在し，局在は不明ながら特殊な環境下においては胚葉を越えた分化能をもつ細胞が表皮に存在することも明らかとなった．

真皮の多能性幹細胞

2001年Tomaらは，マウスの真皮に神経や平滑筋や脂肪細胞に分化できる多能性幹細胞が存在することを示した[4]．神経幹細胞の培養法であるneurosphere法に準じて真皮の細胞を浮遊培養することにより細胞塊(sphere)を形成させ，接着培養に移して分化を誘導するものである．

著者らもマウスで追試に成功し(図1)，細胞凝集を起こさない条件下でもたしかに1個の細胞からクローナルにsphereが増殖すること，TGF-β(transforming growth factor-β)添加によりsphereの形成が促進されること，月齢に従ってsphereの形成率は低下することなどをあらたに報告した[5]．現在，特定の神経細胞が誘導できるかを*in vivo*と*in vitro*で精力的に検討しているところである．

脂肪組織の多能性幹細胞

やはり2001年にZukらは，美容的に脂肪吸引されたヒト脂肪組織のなかに，骨や軟骨や筋肉，神経などに分化する能力のある細胞が存在することを報告した[6]．この細胞は骨髄中に存在する間葉系幹細胞とほぼ同等の多分化能を有するが，骨髄より容易に採取でき，かつ増殖能力も高いので，臨床応用しやすいという利点がある．現在さらなる研究が進みつつあり，幹細胞ソースとして重要な役割を果たすと思われる．

おわりに

以上より，皮膚にはバルジ領域の細胞のように皮膚のなかで多分化能を示す場合と皮膚から取り出して*in vitro*の培養環境のなかで多分化能(細胞の可塑性)を示す細胞が存在することが証明された．細胞が培養という人工的な条件下で脱分化あるいは分化のリセットを起こすのか，もともと未分化な細胞であったのかについては今後の検討が必要である．いずれにしても外胚葉系の表皮細胞から間葉

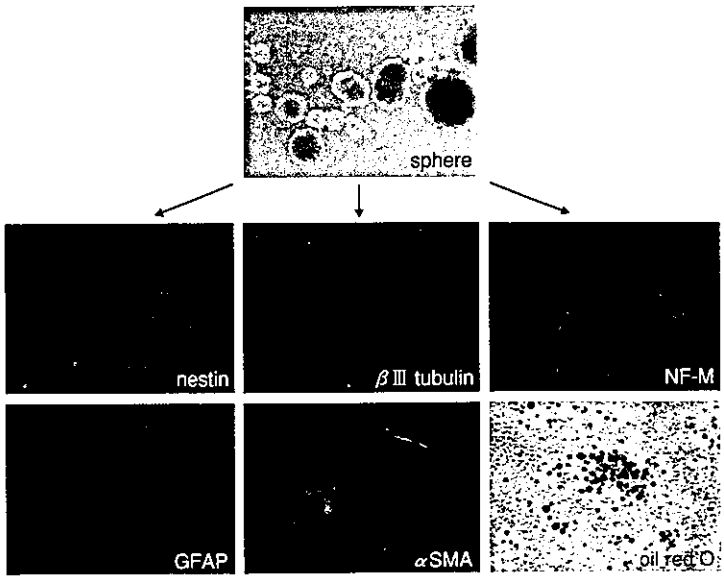

図1　真皮の多能性幹細胞

皮膚の細胞を浮遊培養してsphereを形成させた後，分化条件にするとβIIIチュブリン，neurofilament-M陽性の神経細胞やGFAP陽性のグリア細胞，smooth muscle actin陽性の平滑筋細胞，oil red O染色陽性の脂肪細胞が出現する．

系の筋細胞へ分化したり，間葉系の細胞が神経に分化したりと，いままで不可能と思われていたことが現実に起こりうるわけで，細胞生物学上のパラダイム転換といえる．皮膚から神経細胞やグリア細胞が誘導できれば神経疾患の治療に役立てることができる．とくに自己の細胞という点で，胎児細胞を使用する場合の倫理的な問題は回避でき，ES細胞を使用する場合の腫瘍形成や拒絶反応の問題をクリアできることになる．今後，神経領域のみならず骨や軟骨など他の領域への応用も期待できるので，皮膚の細胞を利用した新しい再生医療が発展すると思われる．

1) Oshima, H. et al.：Morphogenesis and renewal of hair follicles from adult multipotent stem cells. *Cell*, **104**：233-245, 2001.
2) Liang, L. and Bickenbach, J. R.：Somatic epidermal stem cells can produce multiple cell lineages during development. *Stem Cells*, **20**(1)：21-31, 2002.
3) Montanaro, F. et al.：Skeltal muscle engraftment potential of adult mouse skin side population cells *Proc. Natl. Acad. Sci. USA*, **100**：9336-9341, 2003.
4) Toma, J. G. et al.：Isolation of multipotent adult stem cells from the dermis of mammalian skin. *Nat. Cell Biol.*, **3**：778-784, 2001.
5) Kawase, Y. et al.：Characterization of multipotent adult stem cells from the skin：transforming growth factor-β (TGF-β) facilitates cell growth. *Exp. Cell Res.*, **295**(1)：194-203, 2004.
6) Zuk, P. A. et al.：Multilineage cells from human adipose tissue：Implications for cell-based therapies. *Tissue Engineering*, **7**：211-228, 2001.

大河内仁志／Hitoshi OKOCHI
国立国際医療センター研究所
細胞組織再生医学研究部

腎臓内科学

腎病変に果たすインテグリンの役割

The role of integrin in the development of kidney disease

近年，細胞と細胞外基質(ECM)間の接着をつかさどるECMレセプター，β1-インテグリン(IG)ファミリーが，増殖因子，サイトカイン，アンジオテンシンなどの可溶性の腎炎進展因子とともに，腎病変形成にかかわる多彩な細胞動態〔細胞増殖，生存，移動，上皮-間葉移行(EMT)，ECM構築〕を制御していることがしだいに明らかになってきた．そこで本稿では，β1-IGファミリーの腎病変における役割と，そのレセプター機能を制御している細胞内シグナル経路の最新の知見について，著者らの研究成果も含めて紹介する．

腎病変形成における β1-IGファミリーの役割

著者らは，ラットThy-1腎炎にコラーゲンレセプターであるα1β1-IGの機能阻害抗体を腎炎発症3日目に投与すると，腎炎1週目でコントロール抗体投与群と比較して有意にメサンギウム細胞(MC)増殖やECMの蓄積が減少することを見出した[1]．その後，半月体形成性腎炎モデルであるWKYマスギ腎炎でも同阻害抗体を投与すると糸球体硬化や間質の線維化が抑制されることも証明されている．したがって，α1β1-IGは腎炎におけるMC増殖やECM蓄積に重要な働きをしているといえる．また，ヒト腎炎においても，α1β1，α5β1-IG(フィブロネクチンレセプター)の発現とIGのリガンドECMの蓄積のレベルが相関していることも報告されており，腎炎進行にかかわる病的なメサンギウムのECM蓄積にβ1-IGファミリーの発現状態が関与していることを示唆している．

最近，β1-IGファミリーの機能を制御しているシグナル分子のなかで，integrin-linked kinase(ILK)が腎病変形成に必要な細胞動態の調節に重要な役割を果たしていることを示す報告があいついでいる．ILKは，β1，β3鎖にリンクするセリン/スレオニンキナーゼであり，その活性は下流のPKB/Akt，GSK-3，β-catenin，MAPキナーゼ活性を調節している．Kretzlerらは先天性ネフローゼの糸球体ではILK発現が上昇していることを発見し，蛋白尿を呈する腎炎モデルでもILK発現の上昇があり，ポドサイト特異的にILKが増加することを報告した．さらに彼らは，培養ポドサイトは

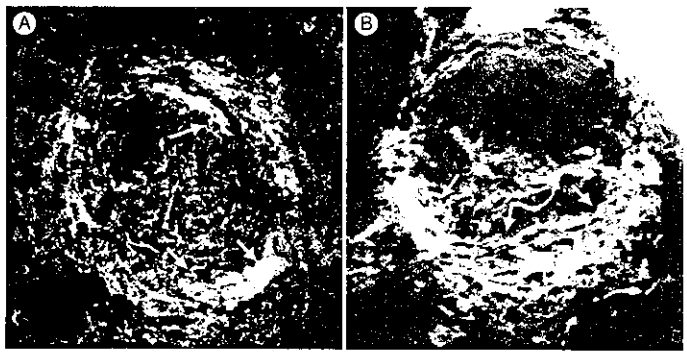

図1　半月体細胞におけるILKとα-SM actinの発見
ラットWKYマスギ腎炎における半月体細胞(矢印)には，ILK(A)やα-SM actin(B)が同時に強く発現している．

ダメージを受けるとILKの発現・活性が上昇し，ILK過剰発現ポドサイトはα3β1-IGを介したコラーゲン基質との接着能が低下することを証明した．種々の原因によるポドサイトダメージは，細胞内ILKの活性化を誘導しα3β1-IGのaffinity, avidityが減弱してポドサイトの基底膜からの剥離を引き起こすことになる[2]．服部らは，移植後再発した巣状糸球体硬化症の患児の血清は，MCNSを含む他の腎疾患患児の血清に比べてポドサイトのILK活性，発現を特異的に上昇させる因子を有していることを見出しており，巣状糸球体硬化症の発症原因を考えるうえで興味深い[3]．一方Guoらは，糖尿病性腎症で糸球体メサンギウムのILKの増加とECMの増加が相関し，高血糖培養ではMCのILK発現が増加してフィブロネクチン線維の集積が上昇することを示した．加えて彼らは培養系でのILK発現誘導実験より，MCのILKがフィブロネクチン基質の組み立てや細胞増殖を制御していることを証明した[4]．著者らもラットの進行性腎炎モデルにおいて，糸球体細胞のILK活性・発現が腎炎進行とともに増加しメサンギウム基質の蓄積増加レベルと関係していることを確認している．*in vivo*でILKが腎炎のECM構築を制御していることをうかがわせる所見である[5]．

ごく最近，Liuらは閉塞性腎症や糖尿病性腎症モデルを用いて，腎線維症(間質線維化)の発症には尿細管上皮細胞にILKが発現誘導されることによりEMTが生じmyofibroblast化したもの(α-SM actin陽性)が関与する機序があることを解明した．さらに，このILK発現誘導にはTGF-βが重要な役割を果たしていることも示した[6]．現在，著者らは，腎炎における半月体形成にもBowman嚢上皮細胞によるILK発現誘導を介したEMTが関与することを示すデータを得ている(図1)[7]．

おわりに

IGが担う細胞接着能と細胞内シグナル伝達経路は腎病変形成に重要な働きをしている．今後，細胞が発現するIGのレパートリーとそれぞれのIGシグナルの全貌が解明され，ILKなどを代表とするシグナル分子の活性，機能を特異的に阻害する薬剤(シグナル阻害薬)が開発されてくると思われる．そのような薬物を用いた慢性・進行性腎炎の新しい治療法の発展が期待される．

1) Kagami, S. et al.：Effects of anti-α1 integrin subunit antibody on anti-Thy-1 glomerulonephritis. *Lab. Invest.*, **82**：1219-1227, 2002.
2) Kretzler, M. et al.：Integrin-linked kinase as a candidate downstream effector in proteinuria. *FASEB J.*, **15**：1843-1845, 2001.
3) Hattori, M. et al.：Induction of integrin-linked kinase(ILK)in mouse cultured podocytes after stimulation with plasma from recurrent-focal segmental glomerulosclerosis patients. *J. Am. Soc. Nephrol.*, **14**：375A, 2003.
4) Guo, L. et al.：The distribution and regulation of integrin-linked kinase in normal and diabetic kidneys. *Am. J. Pathol.*, **159**：1735-1742, 2001.
5) Kagami, S. et al.：Up-regulation of integrin-linked kinase(ILK) activity in the rat mesangioproliferative glomerulonephritis(GN). *J. Am. Soc. Nephrol.*, **13**：500A, 2002.
6) Liu, Y.：Epithelial to mesenchymal transition in renal fibrogenesis：Pathological significance, moleculat mechanism, and therapeutic intervention. *J. Am. Soc. Nephrol.*, **15**：1-12, 2004
7) Shimizu, M. et al.：Enhanced expression of integrin-linked kinase(ILK)in crescent formation in experimental progressive glomerulonaphritis(GN). *J. Am. Soc. Nephrol.*, **14**：630A, 2003.

香美祥二／Shoji KAGAMI
徳島大学大学院ヘルスバイオサイエンス研究部発生発達医学講座小児医学分野

消化器外科学

血小板は肝再生を促進する

Platelets promote liver regeneration

肝再生についてはTNF-αやIL-6などのサイトカイン，hepatocyte growth factor(HGF)などの増殖因子を中心に，これまで多くの研究がなされてきたが，いまだにそのメカニズムの詳細は明らかになっていない．また，これらのサイトカインや増殖因子を，肝再生促進のために劇症肝不全や肝切除後の治療に用いる試みは実験段階にとどまっており，実用化には至っていない．近年，血小板が止血以外にさまざまな機能をもつことが明らかになってきている．

血小板に含まれる肝再生に関連した成分

肝切除後の肝再生にIL-1β，IL-6，TNF-αなどの炎症性サイトカイン，c-jun，c-fosなどの初期応答遺伝子，HGF，epidermal growth factor(EGF)などの増殖因子が深く関与していることが報告されている[1]．血小板には肝再生に必要と考えられているさまざまな因子が含まれており，代表的なものとしてIL-1βがあげられる．IL-1βはmRNAの形で血小板のpolysomeに内包され，刺激を受けると急速に血小板内で蛋白合成が起こり，血小板膜表面に活性型のIL-1βが出現する[2]．初期応答遺

Smart Polyion Complex Micelles for Targeted Intracellular Delivery of PEGylated Antisense Oligonucleotides Containing Acid-Labile Linkages

Motoi Oishi,[a] Fumi Nagatsugi,[b] Shigeki Sasaki,[b] Yukio Nagasaki,*[a, d] and Kazunori Kataoka*[c]

A novel pH-sensitive and targetable antisense ODN delivery system based on multimolecular assembly into polyion complex (PIC) micelles of poly(L-lysine) (PLL) and a lactosylated poly(ethylene glycol)–antisense ODN conjugate (Lac-PEG–ODN) containing an acid-labile linkage (β-propionate) between the PEG and ODN segments has been developed. The PIC micelles thus prepared had clustered lactose moieties on their peripheries and achieved a significant antisense effect against luciferase gene expression in HuH-7 cells (hepatoma cells), far more efficiently than that produced by the nonmicelle systems (ODN and Lac-PEG–ODN) alone, as well as by the lactose-free PIC micelle. In line with this pronounced antisense effect, the lactosylated PIC micelles showed better uptake than the lactose-free PIC micelles into HuH-7 cells; this suggested the involvement of an asialoglycoprotein (ASGP) receptor-mediated endocytosis process. Furthermore, a significant decrease in the antisense effect (27% inhibition) was observed for a lactosylated PIC micelle without an acid-labile linkage (thiomaleimide linkage); this suggested the release of the active (free) antisense ODN molecules into the cellular interior in response to the pH decrease in the endosomal compartment is a key process in the antisense effect. Use of branched poly(ethylenimine) (B-PEI) instead of the PLL for PIC micellization led to a substantial decrease in the antisense effect, probably due to the buffer effect of the B-PEI in the endosome compartment, preventing the cleavage of the acid-labile linkage in the conjugate. The approach reported here is expected to be useful for the construction of smart intracellular delivery systems for antisense ODNs with therapeutic value.

Introduction

Antisense oligodeoxynucleotides (ODNs) have attracted much attention as a class of therapeutic agents that can be used to target mRNA for specific inhibition of gene expression.[1] Nevertheless, the therapeutic value of antisense ODNs under in vivo conditions has not been fully proven to be effective owing to several obstacles, including nonspecific interaction with plasma protein,[2] low stability against enzymatic degradation,[3] low permeability across the cell membrane,[4] and preferential liver and renal clearance.[3] Therefore, a high dose of the antisense ODN is generally required to achieve a significant antisense effect in vivo. To obtain the desired antisense effect, a variety of antisense ODN delivery systems such as cationic lipids (lipoplexes)[5] and cationic polymers (polyplexes)[6] have been developed, and some of these systems contribute substantially to ODN stability against enzymatic degradation and increased cellular uptake, at least under in vitro conditions. However, due to the nonspecific nature of interactions of cationic components with negatively charged biomacromolecules, they often tend to show nonspecific disposition characteristics and short circulating lifetimes in the blood after systemic injection.[7] Recently, a new class of antisense ODN delivery systems has emerged based on polyion complex (PIC) micelles composed of PEG–polycation block copolymers (PEG = poly(ethylene glycol)) and oppositely charged antisense ODNs, held together by electrostatic interactions.[8] The PIC micelles exhibited excellent solubility in aqueous media, high tolerance of entrapped ODNs against enzymatic degradation, and minimal interaction with negatively charged biomacromolecules and cell membrane, owing to the steric stabilization of the very dense PEG corona surrounding the PIC core. However, electrostatic

[a] *Dr. M. Oishi, Prof. Dr. Y. Nagasaki*
Department of Materials Science and Technology
Tokyo University of Science
2641 Yamazaki, Noda, Chiba 278-8510 (Japan)
Fax: (+81) 4-7123-8878
E-mail: nagasaki@ims.tsukuba.ac.jp

[b] *Prof. Dr. F. Nagatsugi, Prof. Dr. S. Sasaki*
Graduate School of Pharmaceutical Science
Kyushu University
3-3-1 Maidashi, Higashi-ku, Fukuoka 812-8582 (Japan)

[c] *Prof. Dr. K. Kataoka*
Department of Materials Science and Engineering
Graduate School of Engineering, The University of Tokyo
7-3-1 Hongo, Bunkyo-ku, Tokyo 113-8656 (Japan)
Fax: (+81) 3-5841-7139
E-mail: kataoka@bmw.t.u-tokyo.ac.jp

[d] *Prof. Dr. Y. Nagasaki*
Current address:
Tsukuba Research Center for Interdisciplinary Materials Science
University of Tsukuba, Tsukuba 305-8573 (Japan)

interaction between PEG–polycation block copolymer and antisense ODN seems to be weak under extremely dilute conditions, due to the low molecular weight of the antisense ODN, with this often leading to the dissociation of the PIC micelles below the critical association concentration (cac). Therefore, the stability of the PIC micelles used for entrapping the antisense ODNs needs to be further improved for use in systemic ODN delivery. On the other hand, the smooth and efficient release of entrapped antisense ODNs from PIC micelles into the intracellular environment after their trafficking into the target cells is needed to achieve an antisense effect.

Recently, our group[9] and Park et al.[10] have independently reported novel PIC micelles composed of an alternative combination of an anionic PEG–ODN conjugate bearing an acid-labile linkage between the PEG and the antisense ODN segment and a polycation of appreciable molecular weight. Improved stability of the PIC micelles is to be expected from this approach, due to the increased association force of the entrapped polycations of appreciable molecular weight. In addition to showing resistance against enzymatic degradation and minimal interaction with negatively charged biomacromolecules, the PEG–ODN/polycation PIC micelles underwent cleavage of the acid-labile linkages between PEG and antisense ODN segments in response to the endosomal pH, which is known to be 1.4–2.4 units lower than that found under standard physiological conditions.[11] The detachment process of the PEG segment in response to the pH decrease in the endosomal compartment would be expected to correspond to the transport of the free (active) antisense ODN moiety from endosome to cytoplasm. Nevertheless, PEG–ODN/polycation PIC micelles may show reduced cellular uptake due to limited interaction between the PEG shell of the micelle and the cell membrane, so installation of specific ligand molecules on the surfaces of the PEG–ODN/polycation PIC micelles is indispensable in order to achieve specific and enhanced cellular uptake through receptor-mediated endocytosis, allowing the effective dose of antisense ODN to be reduced.

Here we wish to report the preparation and bioactivity of pH-sensitive lactosylated PIC micelles composed of a lactosylated PEG–ODN conjugate (Lac-PEG-ODN) bearing an acid-labile linkage between PEG and ODN segments and poly(L-lysine) (PLL), as shown in Figure 1. The lactose moieties on the surfaces of the PIC micelles act as a specific ligand for hepatocytes (liver cells), because hepatocytes are known to have an abundance of asialoglycoprotein (ASGP) receptors that recognize and internalize glycoproteins bearing terminal lactose moieties.[12] The lactosylated PIC micelles could potentially be expected to show enhanced antisense effects relative to PIC micelles without lactose moieties, due to the enhancement of cellular uptake through ASGP receptor-mediated endocytosis.

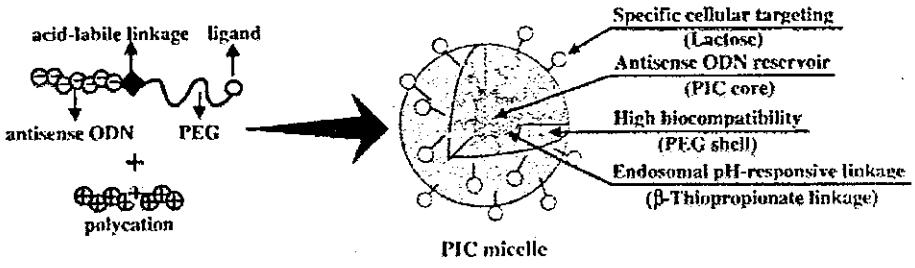

Figure 1. Illustration of the PIC micelle.

Results and Discussion

Synthesis of the lactosylated poly(ethylene glycol)–oligodeoxynucleotide (Lac-PEG-ODN) conjugate

A synthetic route to Lac-PEG-ODN conjugate is shown in Scheme 1. A heterobifunctional PEG bearing an allyl group at the α-end and a hydroxy group at the ω-end (Ally-PEG-OH) was synthesized by anionic ring-opening polymerization of ethylene oxide with use of the allyl alcohol/potassium/naphthalene initiator system.[13] The radical addition of 3-mercaptopropionic acid to the Allyl-PEG-OH in the presence of AIBN quantitatively afforded a carboxylic acid-PEG-OH (HOOC-PEG-OH), which was in turn converted into a HOOC-PEG-Acrylate by treatment with acryloyl chloride in the presence of triethylamine. According to SEC and ^{1}H NMR analyses (Figure 2), the molecular weight of the HOOC-PEG-Acrylate (SEC: M_n=4450, M_w/M_n=1.04 and ^{1}H NMR: M_n=4630) agrees with the calculated molecular weight (calcd. M_n=5060), and a carboxylic acid group and an acrylate group were shown to have been quantitatively introduced at the α-end and the ω-end of the PEG, respectively. The quantitative introduction of a lactose group at the carboxylic acid end of the HOOC-PEG-Acrylate was also performed by treatment with excess 4-aminophenyl β-D-lactopyranoside in the presence of 1-ethyl-3-(3-dimethylaminopropyl)carbodiimide hydrochloride (EDC) and *N*-hydroxysuccinimide (NHS). A ^{1}H NMR spectrum of the Lac-PEG-Acrylate is shown in Figure 3 with assignments, the peaks of aromatic residue assignable to 4-aminophenyl β-D-lactopyranoside moiety being clearly observable at δ=7.14 and 7.34 ppm, along with the acrylate peaks at δ=5.83–6.54 ppm. From the integral ratios between aromatic peaks and acrylate peaks or PEG backbone peaks at 3.65 ppm, it was confirmed that the lactose moiety had been quantitatively introduced at the PEG end. To obtain a Lac-PEG-ODN conjugate bearing an acid-labile linkage (β-thiopropionate linkage), a Michael reaction between the 3′-thiol-modified antisense ODN (5′-ATG CCC ATA CTG TTG AG–$CH_2CH_2CH_2SH$, firefly luciferase, pGL3-control antisense sequence[14]) and excess Lac-PEG-Acrylate (10 equiv) was carried out according to our previous report.[9] For the controls, Ace-PEG-ODN conjugate bearing an acetal group at the PEG end and Lac-PEG-scrODN conjugate bearing a scrambled ODN sequence were also synthesized. Furthermore, a Lac-PEG-Mal-ODN conjugate with no acid-labile linkage between PEG and ODN segments was synthesized through a Michael reaction between Lac-PEG-Maleimide and the 3′-thiol-modified ODN, as shown in Scheme 1.

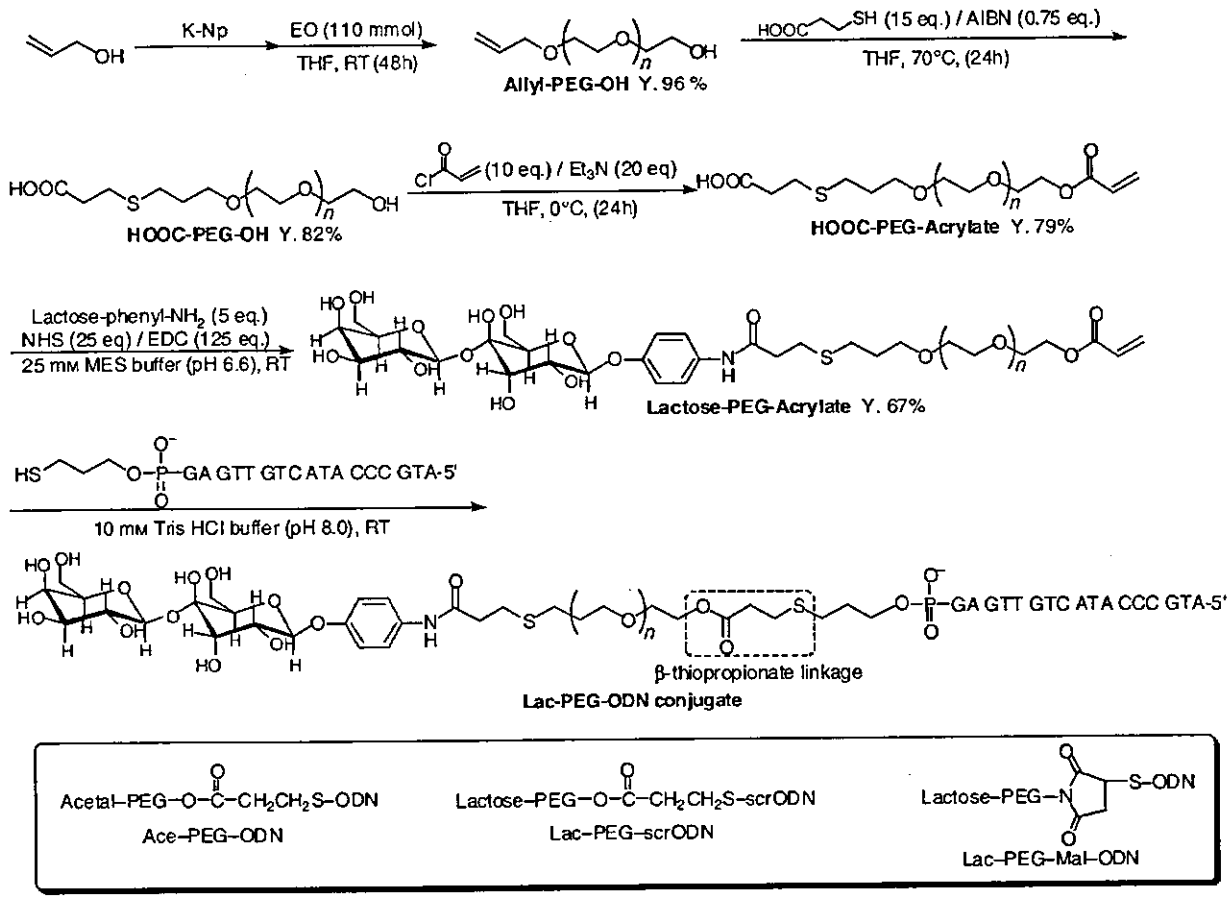

Scheme 1. Synthetic route to Lac-PEG-ODN.

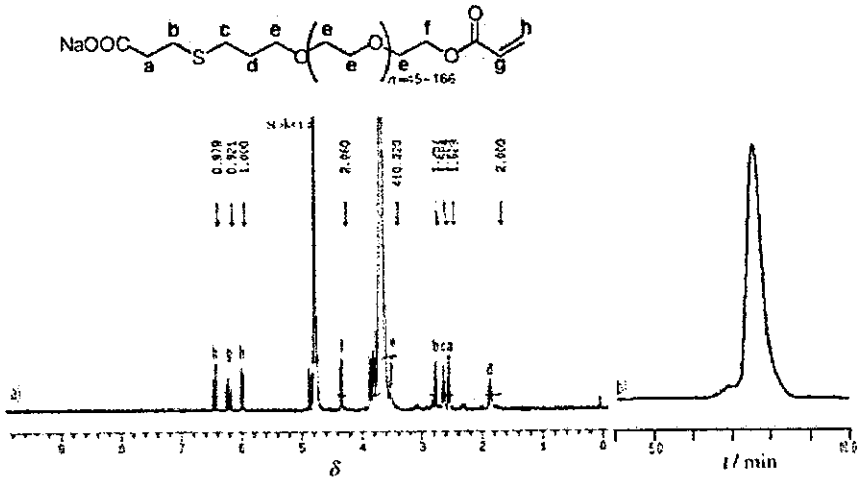

Figure 2. a) ^{1}H NMR spectrum, and b) SEC chromatogram of HOOC-PEG–acrylate.

Cellular association and internalization of the PIC micelles

The obtained Lac-PEG-ODN conjugate would be expected to form a PIC micelle through electrostatic interaction on mixing with the appropriate polycation, as illustrated in Figure 1. ω-FITC-labeled (FITC = fluorescein isothiocyanate) Lac-PEG-ODN conjugate and ω-FITC-labeled Ace-PEG-ODN conjugate were separately mixed with PLL (degree of polymerization (DP) = 460, M_w = 75900) with an equal unit molar ratio of the phosphate group in the PEG–ODN conjugate and amino group in PLL (N/P = 1) to form the FITC-labeled PIC micelles. The fluorescence from the Lac-PEG-ODN-FITC/PLL PIC micelles and Ace-PEG-ODN-FITC/PLL PIC micelles was viewed under a fluorescence microscope at different time intervals (30 and 120 min) after their addition to cultured HuH-7 cells in the presence of 10% fetal bovine serum (FBS) (Figure 4). Note that HuH-7 cells express quite a few ASGP receptors that recognize and internalize compounds bearing terminal lactose moieties. The association of the Lac-PEG-ODN-FITC/PLL PIC micelles with the HuH-7 cells and their internalization were observed as early as after 30 min of incubation, and

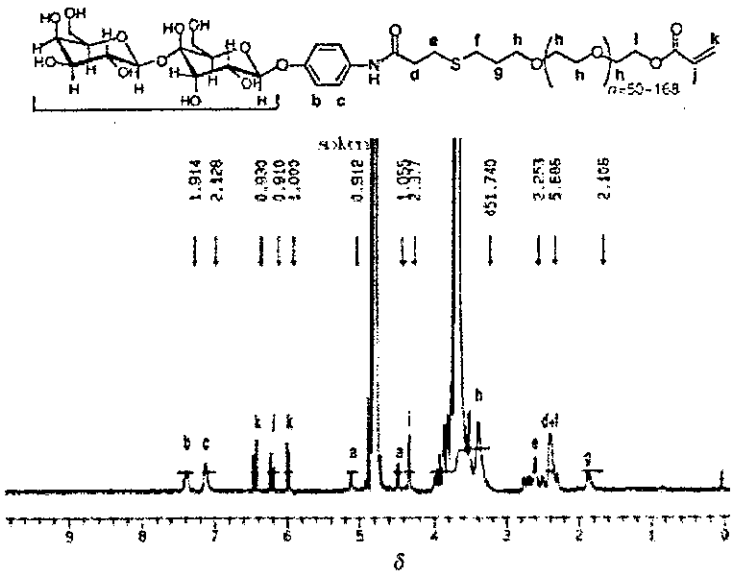

Figure 3. ^1H NMR spectrum of lactose-PEG–acrylate.

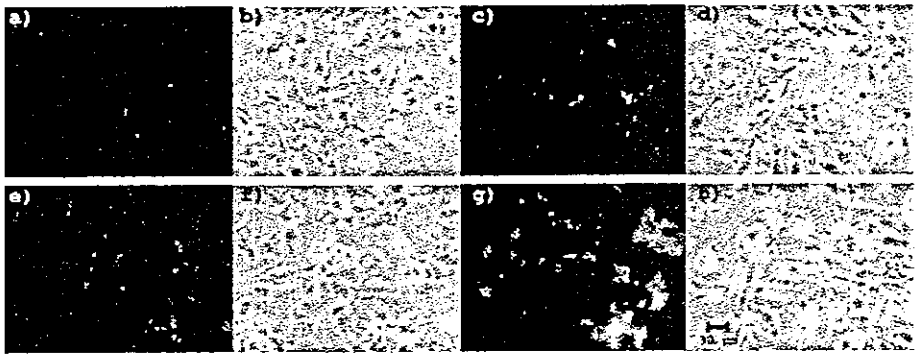

Figure 4. Association and internalization of the Ace-PEG-ODN-FITC/PLL PIC micelles (N/P = 1) and Lac-PEG-ODN-FITC/PLL PIC micelles (N/P = 1) in HuH-7 cells after 30 or 120 min incubation. The PIC micelles used and the incubation time were as follows: a), b) Ace-PEG-ODN-FITC/PLL PIC micelle, 30 min. c), d) Ace-PEG-ODN-FITC/PLL PIC micelle, 120 min. e), f) Lac-PEG-ODN-FITC/PLL PIC micelle, 30 min. g), h) Lac-PEG-ODN-FITC/PLL PIC micelle, 120 min. a, c, e, and g are fluorescent images, and b, d, f, and h are phase-contrast images.

furthermore, the number of fluorescence staining cells and the fluorescence intensity of each staining cell increased with prolongation of incubation time from 30 min to 120 min (26%→ 49% fluorescence positive cells). In contrast, low cellular association of Ace-PEG-ODN-FITC/PLL PIC micelles with HuH-7 cells and low internalization into them was observed even at 120 min (21% fluorescence-positive cells). This result strongly suggests that cellular association and internalization of a Lac-PEG-ODN-FITC/PLL PIC micelle may occur by an ASGP receptor-mediated process, whereas Ace-PEG-ODN-FITC/PLL PIC micelles are taken up into cells only by fluid-phase endocytosis, known to be a substantially slower process than receptor-mediated endocytosis.[15]

Antisense activity of the PIC micelles evaluated by dual luciferase reporter assay

To evaluate the antisense efficiency of the Lac-PEG-ODN in the PIC micelle delivery system, we carried out a dual luciferase reporter assay in HuH-7 cells. Open and closed bars in Figure 5 show the antisense effects of Ace-PEG-ODN/PLL and Lac-PEG-ODN/PLL PIC micelles (N/P = 1, PLL; DP = 460, M_w = 75 900), respectively, in the presence of 10% FBS as a function of the concentration of the conjugate. As the conjugate concentration increases, firefly luciferase expression of the cells treated with Ace-PEG-ODN/PLL PIC micelles ,or Lac-PEG-ODN/PLL micelles was progressively reduced in dose-dependent manner ($^*P < 0.05$). It was also noticed that the antisense effect of the Lac-PEG-ODN/PLL PIC micelles was approximately 1.5 times higher than that of Ace-PEG-ODN/PLL micelles at 5 and 10 μM ($^*P < 0.05$). When asialofetuin (ASF), a natural glycoprotein ligand for the ASGP receptor, was preincubated with the cells (10 mg mL^{-1}) for 30 min before the addition of the Lac-PEG-ODN/PLL PIC micelle, the antisense effect was reduced significantly even at 10 μM: from 65% inhibition to 38% inhibition (hatched bar 1), the same level as achieved by Ace-PEG-ODN/PLL micelles. Since the ASF is known to act as an inhibitor of ASGP receptor-mediated endocytosis,[16] it is likely that an appreciable fraction of the Lac-PEG-ODN/PLL PIC micelle may be taken up into HuH-7 cells by an ASGP receptor-mediated endocytosis process to achieve pronounced antisense activity in relation to that produced by Ace-PEG-ODN/PLL micelles without any particular affinity toward cellular receptors.

It is worth noting that no reduction in firefly luciferase expression was observed even at 10 μM for Lac-PEG-scrODN/PLL PIC micelle (hatched bar 4), a micelle containing a conjugate of scrambled ODN sequence, indicating that inhibition of firefly luciferase expression by the Lac-PEG-ODN/PLL PIC micelles is indeed a sequence-specific event. Non-micelle systems—the 3′-unmodified antisense ODN alone (hatched bar 2) and Lac-PEG-ODN conjugate alone (hatched bar 3)—failed to inhibit the firefly luciferase expression even at high concentrations (up to 10 μM). This may be explained either by a much more rapid enzymatic degradation of antisense ODN and PEG–ODN conjugate in the medium, relative to the PIC micelle,[9] or by impaired diffusivity of naked antisense ODN and Lac-PEG-ODN conjugate, with their negatively charged and hydrophilic characters, through the nega-

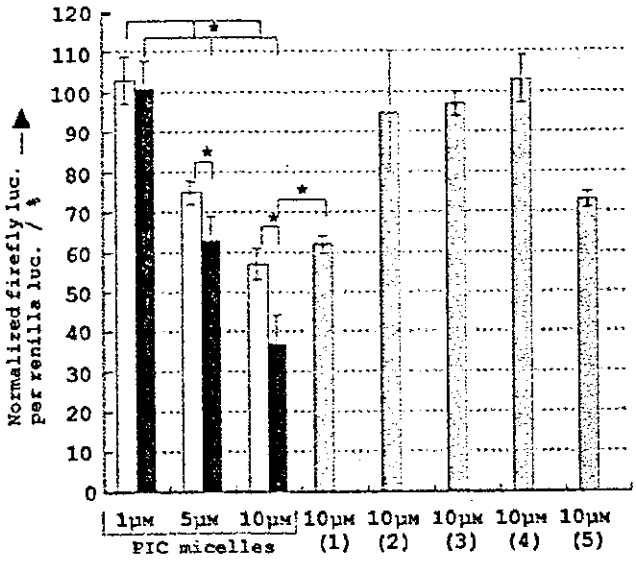

Figure 5. Antisense effects against firefly luciferase gene expression in cultured HuH-7 cells. Open and closed bars show results for the Ace-PEG-ODN/PLL PIC micelles and the Lac-PEG-ODN/PLL PIC micelles, respectively, at varying concentrations. Hatched bars are results for: 1) Lac-PEG-ODN/PLL PIC micelle at 10 μM with ASF, 2) antisense ODN alone at 10 μM, 3) Lac-PEG-ODN conjugate alone at 10 μM, 4) Lac-PEG-scrODN/PLL PIC micelle at 10 μM, and 5) Lac-PEG-Mal-ODN/PLL PIC micelle at 10 μM. Normalized ratios between the firefly luciferase activity (firefly luc.) and the renilla luciferase activity (renilla luc.) are shown in the ordinate. The indicated concentrations of conjugate and antisense ODN were the final concentrations in the total transfection volume (250 μL). The data are shown as the averages from triplicate experiments ±SD. $P^* < 0.05$.

tively charged cell membrane. It should also be noted that the Lac-PEG-Mal-ODN/PLL micelle, a micelle containing the conjugate with a non-acid-labile linkage,[17] was less effective than the Lac-PEG-ODN/PLL PIC micelle: the former showed 27% inhibition (hatched bar 5), whereas the latter achieved 65% inhibition at 10 μM (closed bar). The significant difference in antisense effects between Lac-PEG-ODN/PLL PIC micelle and Lac-PEG-Mal-ODN/PLL PIC micelle can be ascribed to the difference in the natures of their linkages between PEG and ODN segments. The Lac-PEG-ODN conjugate contains an acid-labile (β-thiopropionate) linkage that is cleavable in the low-pH endosome environment, provoking the release of hundreds of free PEG strands from the PIC micelle to increase the colloidal osmotic pressure within the endosomal compartment,[18] and eventually to induce the swelling and disruption of the endosome. This event may facilitate the transport of free antisense ODN into cytoplasm. On the other hand, the Lac-PEG-Mal-ODN conjugate, bearing a stable thiomaleimide linkage not cleavable in the endosomal compartment, may have no contribution in facilitating endosomal escape through osmotic pressure increase. Furthermore, the presence of PEG strands may restrict the interaction of ODN segments with target mRNA in cytoplasm through steric hindrance, as observed by Moulton et al. for conjugates of antisense phosphorodiamidate morpholino oligomers with peptide.[19] These results indicate that the design of the engineered linkage with programmed sensitivity toward intracellular environment ("smart" PEGylation) is of importance in the successful delivery of the PEG-antisense ODN conjugate.

The effect of the PLL length on the antisense activity of the PIC micelles

The effect of the PLL length (DP) on the antisense effect of the PIC micelles was then examined by comparing PLLs with varying DPs (40, 100, and 460). As can be seen in Figure 6a, a striking effect of PLL length on antisense efficacy of the PIC micelle was observed: micelles prepared from shorter PLL components (DP = 40, Mw = 8300) showed only limited efficacy at 5 μM antisense ODN with a 24 h incubation period ($^*P < 0.05$) relative to those with longer PLLs (DP = 100, Mw = 20900 and 460,

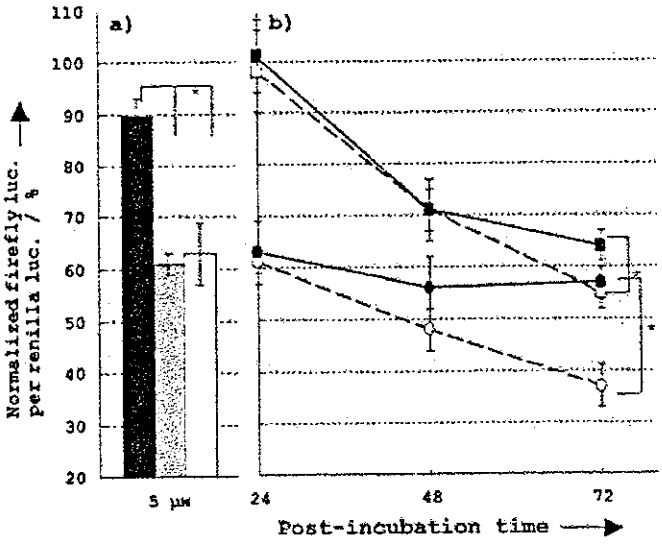

Figure 6. Effect of: a) PLL length (DP = 40 ■, 100 ▪, and 460 □), and b) post-incubation time (24, 48, and 72 h) on the antisense effect of the lactosylated PIC micelles. Normalized ratios between the firefly luc. and the renilla luc. are shown in the ordinate. The final concentrations of conjugate in the total transfection volume (250 μL) were 1 μM (squares) or 5 μM (circles) for DP = 100 (open symbol) or DP = 460 (filled symbol). The data are shown as the averages from triplicate experiments ±SD. $P^* < 0.05$.

Mw = 75900). Presumably the PIC micelles formed from PLL (DP = 40) may be unstable under the extremely dilute conditions ([ODN] ≈ 5 μM) due to the critical dissociation phenomenon, leading to the enzymatic degradation of the Lac-PEG-ODN conjugate. The effect of the incubation time was then further studied for the PIC micelles prepared from the PLLs of DP = 100 and 460. After incubation of HuH-7 cells with PIC micelles for 24 h, the medium was changed to a fresh one free of PIC micelles to continue the culture for a designated time period (24, 48, and 72 h). As can be seen in Figure 6b, both PIC micelles composed of PLL with DP = 100 and DP = 460 (N/P = 1) exhibited an appreciable time-dependent increase in antisense effect even at 1 μM. The antisense effect of the PIC micelle with PLL (DP = 460) reached a constant value after 48 h post-

incubation, whereas that with PLL (DP = 100) exhibited an almost liner increase in antisense effect with the post-incubation time period. Notably, a significant antisense effect was achieved for the PIC micelles with PLL (DP = 100) (45% inhibition at 1 μM and 62% inhibition at 5 μM) after 72 h post-incubation relative to that with PLL (DP = 460) (35% inhibition at 1 μM and 42% inhibition at 5 μM). A lowered antisense effect for the systems with longer PLL (DP = 460) is presumably due to overstabilization of the PIC core, restricting the release of the antisense ODN into the cytoplasm.

The effect of the polycation structure in the PIC core on the antisense activity

To study the effect of the polycation structure in the PIC core on the antisense effects of PIC micelles, branched poly(ethylenimine) (B-PEI, DP = 580, M_w = 25 000) was chosen as the counter polycation, as it has often been used for gene delivery in the form of DNA/B-PEI complexes displaying high transfection efficiency due to the endosomal disruption property of B-PEI (so called "buffer" or "proton-sponge" effect).[20] Nevertheless, the antisense effect of Lac-PEG-ODN/B-PEI PIC micelles (N/P = 1, 9% inhibition at 5 μM and 42% inhibition at 10 μM) was lower than that of Lac-PEG-ODN/PLL micelles (N/P = 1) at 5 and 10 μM ($^*P < 0.05$), as shown in Figure 7. Presumably, the buffer effect of the B-PEI may prohibit the decrease in the endosomal pH,[21] and this should be unfavorable for the cleavage of the acid-labile linkage (β-thiopropionate) of the Lac-PEG-ODN conjugate in the endosome, leading to the release of intact and relatively less active Lac-PEG-ODN conjugate into the cytoplasm.

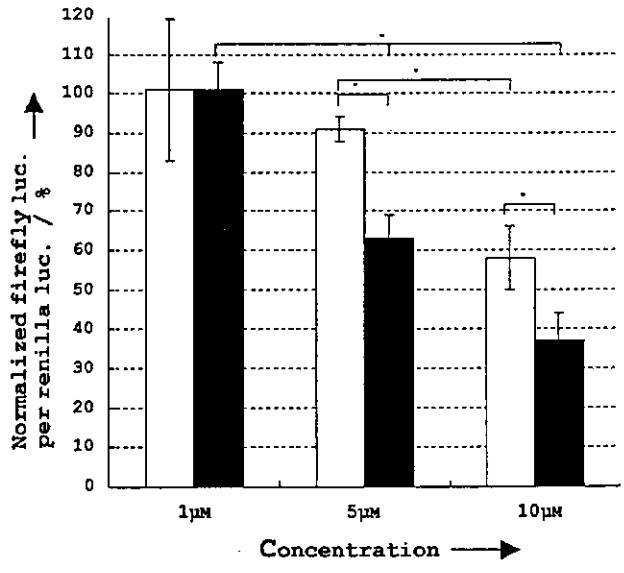

Figure 7. Effect of PIC core polycation structure on the antisense effects of the lactosylated PIC micelles. Normalized ratios between the firefly luc. and the renilla luc. are shown in the ordinate. The indicated concentrations of conjugate were the final concentrations in the total transfection volume (250 μL): □ B-PEI PIC micelles, ■ PLL PIC micelles. The data are shown as the averages from triplicate experiments ± SD. $P^* < 0.05$.

Conclusion

In conclusion, this study reports the preparation of a novel intracellular environment-responsive and targetable antisense ODN delivery system based on the PIC micelle composed of PLL and Lac-PEG-ODN conjugate bearing an acid-labile linkage (β-propionate) between PEG and ODN segments. The lactosylated PIC micelles thus prepared exhibited better association with HuH-7 cells than the lactose-free PIC micelles, as observed by fluorescence microscopy at different time intervals. Delivery of antisense ODN by lactosylated PIC micelle resulted in a significant antisense effect (65% inhibition) for firefly luciferase expression in HuH-7 cells, far more efficient than achieved by using the 3'-unmodified antisense ODN alone (3% inhibition), Lac-PEG-ODN alone (3% inhibition), or lactose-free PIC micelles (45% inhibition), as evaluated by dual luciferase reporter assay. This pronounced antisense effect of the lactosylated PIC micelles indicates that ASGP receptor-mediated endocytosis is considerably involved in the cellular uptake of the lactosylated PIC micelles. Furthermore, a decrease in antisense effect was observed for the lactosylated PIC micelles without any acid-labile linkage (65→27% inhibition), suggesting that cleavage of the acid-labile linkage may occur in response to the lower pH in the endosomal compartment, inducing the efficient release of the active (free) antisense ODN from the PIC core. Such structural parameters—length and type of counter polycation used to make PIC micelles—substantially affected their antisense effects. Significant antisense effects of the PIC micelles (63% inhibition at 5 μM and 45% inhibition at 1 μM) were achieved at 72 h post-incubation time by using PLL with DP = 100, presumably due to the efficient release of antisense ODN from the PIC core through the polyanion exchange reaction in cytoplasm after the detachment of the PEG shell from the PIC micelle in the endosome. All of these results indicate that the system reported here is highly feasible as a smart intracellular delivery system for antisense ODN and related nucleotide compounds for diverse therapeutics.

Experimental Section

Materials: Tetrahydrofuran, ethylene oxide (Sumitomo Seika), allyl alcohol (Wako), triethylamine (Wako), and acryloyl chloride (Wako) were purified by conventional methods. Propan-2-ol, 3-mercaptopropionic acid, 2,2'-azobisisobutyronitrile (AIBN), 1-ethyl-3-(3-dimethylaminopropyl)carbodiimide hydrochloride (EDC), and *N*-hydroxysuccinimide (NHS) were purchased from Wako and were used without further purification. 4-Aminophenyl β-D-lactopyranoside was purchased from Toronto Research Chemicals, Inc. Potassium naphthalene was used as a THF solution, the concentration of which was determined by titration. Water was purified with a Milli-Q apparatus (Millipore). Plasmid DNAs (pDNA) encoding firefly luciferase (pGL3-Control, Promega; 5256 bpa) and renilla luciferase (pRL-TK, Promega; 4045 bpa) were amplified by use of EndoFree Plasmid Maxi or Mega Kits (QIAGEN). The DNA concentration was determined by reading of the absorbance at 260 nm. PLL (DP = 40, M_w = 8300; DP = 100, M_w = 20 900; DP = 460, M_w = 75 900) and B-PEI (DP = 580, M_w = 25 000) were purchased from Sigma and Aldrich, respectively. 3'-Thiol-modified ODNs (5'-ATG CCC ATA CTG TTG AG-$CH_2CH_2CH_2SH$, firefly luciferase, pGL3-control antisense sequence,[14]

and 5'-TCC GTC TAA TGA CGA GT-$CH_2CH_2CH_2SH$, scrambling sequence) were synthesized as in our previous report[9] with a DNA synthesizer (94DNA/RNA Synthesizer, Applied Biosystems).

Polymer analysis: ^{1}H NMR (400 MHz) spectra were obtained in D_2O with a JEOL EX400 spectrometer. Chemical shifts are reported in ppm relative to D_2O ($\delta = 4.79$, ^{1}H). Size exclusion chromatography (SEC) in an organic solvent was performed with a TOSO HLC-8020 apparatus equipped with an internal refractive index (RI) detector (RID-6 A) with a combination of TSK $G4000_{HR}$ and $G3000_{HR}$ columns and THF as the eluent.

Synthesis of HOOC-PEG-OH: Allyl-PEG-OH ($M_n = 4340$, $M_w/M_n = 1.03$) was prepared as in the previous report.[13] Allyl-PEG-OH (4.34 g, 1.0 mmol) was dissolved in anhydrous THF (30 mL), together with 3-mercaptopropionic acid (1.6 g, 15 mmol, 15 equiv) and AIBN (0.123 g, 0.75 mmol, 0.75 equiv), and the resulting mixture was degassed by three freeze–pump–thaw cycles. The radical addition was carried out at 70 °C for 24 h. The polymer was recovered by precipitation in cold propan-2-ol (−15 °C, 2 L) and centrifuged for 45 min at 6000 rpm. Further purification was carried out by dialysis against distilled, deionized water (M_W cutoff 3500), and the product was then freeze-dried to give HOOC-PEG-OH (3.64 g, 82% yield). SEC $M_n = 4330$, $M_w/M_n = 1.04$ (calcd. $M_n = 5010$); ^{1}H NMR (D_2O): $\delta = 1.83$–1.96 (m, 2H; $NaOOCCH_2CH_2$–S–$CH_2CH_2CH_2O$–), 2.57 (t, $J = 7.6$ Hz, 2H; $NaOOCCH_2CH_2$–S–), 2.63 (t, $J = 7.2$ Hz, 2H; $NaOOCCH_2CH_2$–S–$CH_2CH_2CH_2O$–), 2.82 (t, $J = 7.6$ Hz, 2H; $NaOOCCH_2CH_2$–S–$CH_2CH_2CH_2O$–), 3.63 ppm (s, 457H; PEG-backbone)

Synthesis of HOOC-PEG-acrylate: A solution of the HOOC-PEG-OH (2.0 g, 0.45 mmol) and Et_3N (0.911 g, 9.0 mmol, 20 equiv) in THF (15 mL) was added dropwise over 1 h at 0 °C to a mixture of acryloyl chloride (0.400 g, 4.5 mmol, 10 equiv) in THF (5.0 mL). The reaction was allowed to proceed at 0 °C for 24 h in the dark. The polymer was recovered by precipitation in cold propan-2-ol (−15 °C, 1 L) and centrifuged for 45 min at 6000 rpm. Further purification was carried out by dialysis against distilled, deionized water (M_W cutoff 3500) and the product was then freeze-dried to give HOOC-PEG-acrylate (1.60 g, 79% yield). SEC $M_n = 4450$, $M_w/M_n = 1.04$ (calcd. $M_n = 5060$); ^{1}H NMR (D_2O, in Figure 2): $\delta = 1.81$–1.94 (m, 2H; $-H_d$), 2.55 (t, $J = 7.6$ Hz, 2H; $-H_a$), 2.63 (t, $J = 7.2$ Hz, 2H; $-H_c$), 2.80 (t, $J = 7.6$ Hz, 2H; $-H_b$), 3.63 (s, 410H; PEG-backbone, $-H_e$), 4.36 (t, $J = 6.4$ Hz, 2H; $-H_f$), 5.98 (dd, $J = 1.8$, 12.8 Hz, 1H; $-H_h$), 6.23 (dd, $J = 12.8$, 25.4 Hz, 1H; $-H_g$), 6.44 (dd, $J = 1.8$, 12.8 Hz, 1H; $-H_h$).

Lactosylation of HOOC-PEG-acrylate: The HOOC-PEG-acrylate (100 mg, 22 μmol) and 4-aminophenyl β-D-lactopyranoside (48 mg, 111 μmol) were dissolved in MES buffer (25 mM, pH 6.6, 5.0 mL) together with EDC (532 mg, 2.78 mmol, 125 equiv) and NHS (64 mg, 555 μmol, 25 equiv). The reaction mixture was stirred at room temperature for 24 h. The polymer was recovered by precipitation in cold propan-2-ol (−15 °C, 200 mL) and centrifuged for 45 min at 6000 rpm. Further purification was carried out by dialysis against distilled, deionized water (M_W cutoff 3500) and the product was then freeze-dried to give lactose-PEG-acrylate (69 mg, 67% yield). SEC $M_n = 4630$, $M_w/M_n = 1.04$ (calcd. $M_n = 5490$); ^{1}H NMR (D_2O, in Figure 3): $\delta = 1.79$–1.95 (m, 2H; $-H_d$), 2.37–2.41 (m, 4H; $-H_a$, $-H_c$), 2.63 (t, $J = 7.2$ Hz, 2H; $-H_e$), 3.65 (s, 452H; PEG-backbone, $-H_b$), 4.37 (t, $J = 6.4$ Hz, 2H; $-H_f$), 4.46–4.54 (m, 1H; $-H_g$), 5.13–5.19 (m 1H; $-H_g$), 5.98 (dd, $J = 1.8$, 12.8 Hz, 1H; $-H_h$), 6.21 (dd, $J = 12.8$, 25.4 Hz, 1H; $-H_j$), 6.43 (dd, $J = 1.8$, 12.8 Hz, 1H; $-H_k$), 7.14 (d, $J = 7.7$ Hz, 2H; $-H_j$), 7.39 ppm (d, $J = 7.7$ Hz, 2H; $-H_b$).

Synthesis of PEG–ODN conjugates: To obtain a Lac-PEG-ODN conjugate bearing an acid-labile linkage, a Michael reaction of the 3'-thiol-modified ODN with excess lactose-PEG-acrylate (10 equiv) was carried out according to our previous report (79% yield).[9] In addition, three types of PEG–ODN conjugate—possessing an acetal group at the PEG end (Ace-PEG-ODN, 84% yield), a scrambled ODN-sequence (Lac-PEG-scrODN, 88% yield), and a non-acid-labile linkage (Lac-PEG-Mal-ODN, 67% yield)—were also synthesized in the same manner. ^{1}H NMR (for Ace-PEG-ODN conjugate, D_2O): $\delta = 1.19$ (t, $J = 9.4$ Hz, 6H; $-OCH_2CH_3$), 1.73 (t, $J = 7.3$ Hz, 2H; $-SCH_2CH_2COO$–), 1.81–2.33 (m, 36H; 2'-methylene + ODN–$CH_2CH_2CH_2S$–), 2.43 (t, $J = 7.3$ Hz, 2H; $-CH_2CH(OEt)_2$), 3.02–3.16 (m, 4H; $-CH_2SCH_2$–) 3.58 (s, 432H; PEG-backbone + ODN–$CH_2CH_2CH_2S$– + $-OCH_2CH_3$), 3.88–3.94 (m, 36H; 4'-methine + $-COOCH_2$–), 4.16 (s, 34H; 5'-methylene), 4.48 ppm (t, $J = 7.3$ Hz, 1H; $-CH_2CH(OEt)_2$). 1'-Methine protons and 3'-methine protons were overlapped by the peak of H_2O (4.79 ppm).

Preparation of PIC micelle: Specific amounts of the PEG–ODN conjugates and polycations were dissolved in Tris-HCl buffer (10 mM, pH 7.4) to prepare the stock solutions. The solutions were filtered through a 0.1 μm filter to remove the dust. The PEG–ODN conjugate stock solution was mixed with polycation stock solution at an equal unit molar ratio of phosphate group in the PEG–ODN conjugate and amino group in the polycation ($N/P = 1$), followed by the addition of Tris-HCl buffer (10 mM, pH 7.4) including NaCl (0.3 M) to adjust the ionic strength of the solution to physiological conditions (0.15 M NaCl). The size and size distribution of the PIC micelle was elucidated by DLS measurements(DLS-7000, Photal, Otsuka Electronics).[9]

Cell culture: HuH-7 human cancer cells derived from a hepatocarcinoma cell line were obtained from the Cell Resource Center for Biomedical Research, Institute of Development, Aging, and Cancer, Tohoku University. The cells were grown in Dulbecco's modified Eagle's medium (DMEM) supplemented with fetal bovine serum (FBS, 10%), penicillin (100 units mL^{-1}), and streptomycin (100 μg mL^{-1}) at 37 °C in a humidified 5% CO_2 atmosphere.

Fluorescence microscopy: FITC-labeled (FITC = fluorescein isothiocyanate) Lac-PEG-ODN and Ace-PEG-ODN conjugates were prepared from 5'-FITC- and 3'-thiol-modified ODN and lactose-PEG-acrylate. HuH-7 cells were seeded at a density of 5×10^5 cells per dish in a 35 mm glass-bottomed dish (Iwaki, Japan) and kept overnight at 37 °C in a 5% CO_2 atmosphere. The Lac-PEG-ODN-FITC/PLL and Ace-PEG-ODN-FITC/PLL PIC micelles ($N/P = 1$, PLL; DP = 460) were added at a conjugate concentration of 1 μM and incubated at 37 °C in a 5% CO_2 atmosphere for the designated time (30 and 120 min). The cells were washed three times with phosphate buffered saline (PBS) and imaged directly in the cell culture medium with an Olympus IX70 and an appropriate filter.

Dual luciferase reporter assay: HuH-7 cells were plated in a 24-well plate (5×10^4 cells per well) to reach about 50% confluence at transfection. The cells were grown for 24 h and the culture medium was changed to OPIMEM I. The cells were co-transfected with two luciferase plasmids (firefly luciferase, pGL3-control and renilla luciferase, pRL-TK) in the presence of LipofectAMINE (Invitrogen). For each well, pGL3 (0.0835 μg) and pRL (0.75 μg) were applied; the final volume was 250 μL per well. The cells were incubated for 4 h, and the transfection medium was then changed to DMEM with FBS (10%, 225 μL per well). The PIC micelle ($N/P = 1$) (25 μL per well) was added to make up a prescribed concentration. After 24 h incubation, the transfection medium was changed to fresh DMEM with FBS (10%), and the cells were further incubated for the designated time (24, 48, and 72 h). The luciferase expression was monitored with the dual luciferase assay kit (Promega) and ARVOSX-1 (Perkin–Elmer).

Acknowledgements

This work was supported by the Core Research for Evolutional Science and Technology (CREST) of the Japan Science and Technology Agency [JST].

Keywords: antisense agents · bioconjugates · micelles · oligonucleotides · poly(ethylene glycol)

[1] a) S. T. Crooke, *Biotechnol. Genet. Eng. Rev.* **1998**, *15*, 121; b) P. D. Cook, *Handb. Exp. Pharmacol.* **1998**, *131*, 51; c) R. Wagner, *Nature* **1994**, *372*, 323; d) C. A. Stein, Y. C. Cheng, *Science* **1993**, *261*, 1004; e) E. Uhlman, A. Peyman, *Chem. Rev.* **1990**, *90*, 543.

[2] C. A. Stein, *Nat. Med.* **1995**, *1*, 1119.

[3] S. Agrawal, J. Temsamani, W. Galbraith, J. Tang, *Clin. Pharmacokinet.* **1995**, *28*, 7.

[4] P. C. Zamecnik, J. Goodchild, Y. Taguchi, P. S. Sarin, *Proc. Natl. Acad. Sci. USA* **1986**, *83*, 4143.

[5] a) M. Carriere, I. Tranchant, P. A. Niore, G. Byk, N. Mignet, V. Escriou, D. Scherman, J. Herscovici, *J. Liposome Res.* **2002**, *12*, 95; b) L. M. C. de Pedroso, S. Simoes, P. Pires, H. Faneca, N. Duzgunes, *Adv. Drug Delivery Rev.* **2001**, *47*, 277; c) A. D. Miller, *Angew. Chem.* **1998**, *110*, 1862; *Angew. Chem. Int. Ed.* **1998**, *37*, 1768d) R. J. Lee, L. Huang, *Crit. Rev. Ther. Drug Carrier Syst.* **1997**, *4*, 337; e) J.-P. Behr, *Bioconjugate Chem.* **1994**, *5*, 382.

[6] a) T. Merdan, J. Kopecek, T. Kissel, *Adv. Drug Delivery Rev.* **2002**, *54*, 715; b) S. J. Hwang, M. E. Davis, *Curr. Opin. Mol. Ther.* **2001**, *3*, 183; c) R. Kircheis, E. Wagner, *Gene Funct. Dis. Gene Ther. Reg.* **2000**, *1*, 95; d) S. C. De Smedt, J. Demeester, W. E. Hennink, *Pharm. Res.* **2000**, *17*, 113; e) M. C. L. Garnett, *Crit. Rev. Ther. Drug Carrier Syst.* **1999**, *16*, 147.

[7] a) A. V. Kabanov, V. A. Kabanov, *Bioconjugate Chem.* **1995**, *6*, 7; b) I. Jääskeläinen, J. Mönkkönen, A. Urtti, *Biochim. Biophys. Acta* **1994**, *1195*, 115.

[8] a) Y. Kakizawa, A. Harada, K. Kataoka, *Biomacromolecules* **2001**, *2*, 491; b) A. Harada, H. Togawa, K. Kataoka, *Eur. J. Pharm. Sci.*, **2001**, *13*, 35; c) S. V. Vinogradov, T. K. Bronich, A. V. Kabanov, *Bioconjugate Chem.* **1998**, *9*, 805; d) K. Kataoka, H. Togawa, A. Harada, K. Yasugi, T. Matsumoto, S. Katayose, *Macromolecules* **1996**, *29*, 8556; e) A. V. Kabanov, S. V. Vinogradov, Yu. Suzdaltseva, V. Yu. Alakhov, *Bioconjugate Chem.* **1995**, *6*, 639; f) A. Harada, K. Kataoka, *Macromolecules* **1995**, *28*, 5294.

[9] M. Oishi, S. Sasaki, Y. Nagasaki, K. Kataoka, *Biomacromolecules* **2003**, *4*, 1426.

[10] J. H. Jeong, S. W. Kim, T. G. Park, *Bioconjugate Chem.* **2003**, *14*, 473.

[11] J. Gruenberg, *Nat. Immunol. Nat. Rev. Mol. Cell. Biol.* **2001**, *2*, 721.

[12] a) C. H. Wu, G. Y. Wu, *Adv. Drug Delivery Rev.* **1998**, *29*, 243; b) M. Hashida, S. Takemura, M. Nishikawa, Y. Takakura, *J. Controlled Release* **1998**, *53*, 301; c) R. J. Stockert, *Physiol. Rev.* **1995**, *75*, 591.

[13] S. Cammas, Y. Nagasaki, K. Kataoka. *Bioconjugate Chem.* **1995**, *6*, 226.

[14] M. Mishra, J. R. Bennett, G. Chaudhuri, *Biochem. Pharmacol.* **2001**, *61*, 467.

[15] P. E. Stromhaug, T. O. Berg, T. Gjoen, P. O. Seglen, *Eur. J. Cell Biol.* **1997**, *73*, 28.

[16] M. A. Zanta, O. Boussif, A. Adib, J. P. Behr, *Bioconjugate Chem.* **1997**, *8*, 839.

[17] J. H. Jeong, S. W. Kim, T. G. Park, *J. Controlled Release* **2003**, *93*, 183.

[18] S. L. Goh, N. Murthy, M. Xu, J. M. J. Fréchet, *Bioconjugate Chem.* **2004**, *15*, 467.

[19] H. M. Moulton, M. H. Nelson, S. A. Hatlevig, M. T. Reddy, P. L. Iversen, *Bioconjugate Chem.* **2004**, *15*, 290.

[20] O. Boussif, F. Lezoualc, M. A. Zanta, M. D. Mergny, D. Scherman, B. Demeneix, J. P. Behr, *Proc. Natl. Acad. Sci. USA* **1995**, *92*, 7297.

[21] N. D. Sonawane, F. C. Szoka, A. S. Verkman, *J. Biol. Chem.* **2003**, *278*, 44826.

Received: September 16, 2004
Published online on ■■ ■■, 2005

A novel pH-sensitive and targetable antisense ODN delivery system was successfully prepared by assembling lactosylated PEG–antisense ODN conjugates containing acid-labile β-thiopropionate linkages into polyion complex (PIC) micelles through mixing with poly(L-lysine; see figure). The lactosylated PIC micelles enhanced gene silencing in hepatoma cells remarkably; this indicated that this approach is feasible for a targetable antisense ODN delivery system.

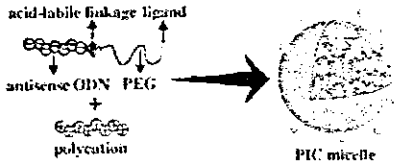

M. Oishi, F. Nagatsugi, S. Sasaki, Y. Nagasaki, K. Kataoka**

■■ – ■■

Smart Polyion Complex Micelles for Targeted Intracellular Delivery of PEGylated Antisense Oligonucleotides Containing Acid-Labile Linkages

Anal. Chem. 2005, *77*, 1075−1080

A Reactive Poly(ethylene glycol) Layer To Achieve Specific Surface Plasmon Resonance Sensing with a High S/N Ratio: The Substantial Role of a Short Underbrushed PEG Layer in Minimizing Nonspecific Adsorption

Katsumi Uchida,[†,‡] Hidenori Otsuka,[§,∥] Mitsuhiro Kaneko,[†] Kazunori Kataoka,[§] and Yukio Nagasaki*[,†,⊥]

Department of Materials Science, Tokyo University of Science, 2641 Yamazaki, Noda-shi, Chiba 270-8510, Japan, and Graduate School of Engineering, The University of Tokyo, 7-3-1 Hongo, Bunkyo-ku, Tokyo 113-8656, Japan

A reactive poly(ethylene glycol) (PEG)-brushed layer was constructed on a surface plasmon resonance (SPR) sensor chip using a heterobifunctional PEG possessing an acetal group at one end and a mercapto group at the other end (α-acetal-ω-mercapto-PEG). The density of the PEG brushed layer substantially increased with repetitive adsorption/rinse cycles of the PEG on the sensor chip, allowing dramatic reduction of nonspecific protein adsorption. Notably, formation of a short, filler layer of PEG (2 kDa) in the preconstructed longer PEG brushed layer (5 kDa) achieved almost complete prevention of nonspecific protein adsorption. The acetal group located at the distal end of the tethered PEG was converted to an aldehyde group by the acid treatment, followed by the installation of biocytin hydrazide through Schiff base formation. SPR sensing of streptavidin was done with a very high S/N ratio even in a proteinous medium using the biotinylated PEG (5 kDa) tethered chip with an inert filler layer of short PEG (2 kDa). Furthermore, the specific affinity of streptavidin for the biotinylated PEG was highly influenced by the length of the filler PEG and was significantly reduced when the length of the filler PEG was longer than that of the biotinylated PEG. This result clearly revealed the substantial importance of the steric factor on biospecific interaction at the distal end of tethered PEG on the sensor surface.

Biosensors for detecting specific biomolecular interactions such as antigen/antibody recognition and DNA hybridization play a significant role as a tool in the biochemical and medical fields. Particularly, a surface plasmon resonance (SPR) analyzer has been widely utilized as a label-free, real-time measurement system.[1−14] Even in the highly sensitive biosensor, the background, viz. nonspecific adsorption of biocomponents often decreases such sensing ability. Thus, to prevent nonspecific adsorption, a variety of modifications on the surface has been carried out.[4,9,15−22] Modification by poly(ethylene glycol) (PEG) tethered chains leads to a significant reduction in the nonspecific interaction of biological molecules with the sensor surface because PEG is highly hydrophilic and has appreciable chain flexibility inducing an effective

* To whom correspondence should be addressed. Telephone: +81-29-853-5749. Fax: +81-29-855-7440. E-mail: nagasaki@nagalabo.jp.

† Tokyo University of Science.

‡ Present address: Department of Applied Chemistry, Tokyo University of Science, 1-3 Kagurazaka, Shinjuku-ku, Tokyo 162-8601, Japan.

§ The University of Tokyo.

∥ Present address: Artificial Organ Materials Research Group, Biomaterials Center, National Institute for Materials Science, 1-1 Namiki, Tsukuba, Ibaraki 305-0044, Japan.

⊥ Present address: Tsukuba Research Center for Interdisciplinary Materials Science, University of Tsukuba, 1-1-1 Tsukuba, Ibaraki 305-8573, Japan.

10.1021/ac0486140 CCC: $30.25
Published on Web 01/15/2005

(1) Liedberg, B.; Nylander, C.; Lungström, I. *Sens. Actuators* **1983**, *4*, 299−304.
(2) Melendez, J.; Carr, R.; Barholomew, D. U.; Kukanskis, K.; Elkind, J.; Yee, S.; Furlong, C.; Woodbury, R. *Sens. Actuators, B* **1996**, *35*, 212−216.
(3) Whelan, R. J.; Wohland, T.; Neumann, L.; Huang, B.; Kobilka, B.; Zare, R. N. *Anal. Chem.* **2002**, *74*, 4570−4576.
(4) Fägerstam, L. G.; Frosell-Karlsson, Å.; Karlsson, R.; Persson, B.; Rönnberg, I. *J. Chromatogr.* **1992**, *597*, 397−410.
(5) Cush, R.; Cronin, J. M.; Stewart, W. J.; Maule, C. H.; Molloy, J.; Goddard, N. J. *Biosens. Bioelectron.* **1993**, *8*, 347−353.
(6) Malmqvist, M.; Karlsson, R. *Curr. Opin. Chem. Biol.* **1997**, *3*, 378−383.
(7) Natsume, T.; Nakayama, H.; Jansson, Ö.; Isobe, T.; Takio, K.; Mikoshiba, K. *Anal. Chem.* **2000**, *72*, 4193−4198.
(8) Gómara, M. J.; Ercilla, G.; Alsina, M. A.; Haro, I. *J. Immunol. Methods* **2000**, *246*, 13−24.
(9) Nakamura, R.; Muguruma, H.; Ikebukuro, K.; Sasaki, S.; Nagata, R.; Karube, I.; Pedersen, H. *Anal. Chem.* **1997**, *69*, 4649−4652.
(10) Bier, F. F.; Kleinjung, F.; Scheller, F. W. *Sens. Actuators, B* **1997**, *38*, 78−82.
(11) Williams, C.; Addona, T. A. *Trends Biotechnol.* **2000**, *18*, 45−48.
(12) McDonnell, J. M. *Curr. Opin. Chem. Biol.* **2001**, *5*, 572−577.
(13) Yu, F.; Knoll, W. *Anal. Chem.* **2004**, *76*, 1971−1975.
(14) Stenberg, E.; Persson, B.; Roos, H.; Urbaniczky, C. *J. Colloid Interface Sci.* **1991**, *143*, 513−526.
(15) Kwok, C. S.; Mourad, P. D.; Crum, L. A.; Ratner, B. D. *Biomacromolecules* **2000**, *1*, 139−148.
(16) Heggli, M.; Tirelli, N.; Zisch, A.; Hubbell, J. A. *Bioconjugate Chem.* **2003**, *14*, 967−973.
(17) Shen, M.; Wagner, M. S.; Castner, D. G.; Ratner, B. D.; Horbett, T. A. *Langmuir* **2003**, *19*, 1692−1699.
(18) Xia, N.; Hu, Y.; Grainger, D. W.; Castner, D. G. *Langmuir* **2002**, *18*, 3255−3262.
(19) Löfås, S.; Johnsson, B.; Edström, Å.; Hansson, A.; Lindquist, G.; Hillgren, R.-M. M.; Stigh, L. *Biosens. Bioelectron.* **1995**, *10*, 813−822.
(20) Roberts, C.; Chen, C. S.; Mrksich, M.; Martichonok, V.; Ingber, D. E.; Whitesides, G. M. *J. Am. Chem. Soc.* **1998**, *120*, 6548−6555.
(21) Holmlin, R. E.; Chen, X.; Chapman, R. G.; Takayama, S.; Whitesides, G. M. *Langmuir* **2001**, *17*, 2841−2850.
(22) Sikavitsas, V.; Nitsche, J. M.; Mountziaris, T. J. *Biotechnol. Prog.* **2002**, *18*, 885−897.

exclusion volume effect.[23-27] The key issue in repelling nonspecific adsorption by tethered PEG is control of the length and density of the PEG.[28-30] However, the length and the density of the tethered PEG layer involve a tradeoff relation. Increase in the PEG chain length to construct a defined tethered chain layer results in a decrease in the density of the PEG chain due to the exclusion volume effect.[31] Construction of a highly dense layer of a substantially longer PEG chain is surely imperative for obtaining a nonfouling sensor surface. To solve this controversial issue of the length and density of the PEG layer, we developed here a novel approach of undercovering the ligand-installed PEG layer with a filler layer of a considerably shorter PEG chain. Another important issue in the construction of a highly sensitive sensor chip is the proper ligand installation. To introduce a ligand installation site at the distal end of the tethered PEG chain, we have developed a novel synthetic heterobifunctional PEG, possessing different functional groups at each chain end, with a controlled molecular weight and a very narrow molecular weight distribution based on anionic ring-opening polymerization of ethylene oxide using various types of metal alkoxide initiators.[32-35] The one used here is α-acetal-ω-mercapto-PEG.[34,35] The mercapto group reacts with the gold surface of the SPR sensor chip, while the acetal group is transformed by an acid treatment to an aldehyde group having high reactivity with the primary amino group of biologically significant molecules as ligands.

EXPERIMENTAL SECTION

Materials. Two lots of α-acetal-ω-mercapto-PEG with different molecular weights were synthesized according to our established method.[33,34] The molecular weight and the molecular weight distribution of the synthesized PEGs, denoted PEG5k and PEG2k, were 4990 and 1.04 and 1920 and 1.03, respectively. A gold chip (SIA KIT Au) for SPR measurement was purchased from Biacore AB (Uppsala, Sweden). Biocytin hydrazide was obtained from Pierce. Streptavidin was obtained from Vector Lab. Bovine serum albumin (BSA) was purchased from Sigma-Aldrich Fine Chemicals. A solution of 0.01 M HEPES buffer (pH 7.4, containing 0.15 M sodium chloride, 3 mM EDTA, and 0.005% surfactant P20) was purchased from Biacore AB (Uppsala, Sweden). As a control, a dextran-modified gold chip (CM5) for SPR measurement was obtained from Biacore AB (Uppsala, Sweden). SPR evaluations were carried out on a Biacore 3000 device (Biacore AB).

Preparation of α-Acetal-ω-mercapto-PEG-Modified Gold Chip. Introduction of hetero-PEG onto the sensor chip surface was carried out using an SPR instrument (Biacore 3000). After a bare gold sensor chip was docked into the instrument, sodium phosphate buffer (pH 7.4, 0.05 M, containing 1 M NaCl) solution of acetal-PEG-SH (1 mg/mL) was injected at a constant flow rate of 20 μL/min for 20 min at 37 °C. After a completed injection, the gold chip was washed with a solution of 0.05 M NaOH for 1 min. This washing was repeated twice in order to increase the introduction efficiency. An SPR sensorgram on the gold sensor chip for this adsorption/rinse of PEG was monitored, and the amount of tethered PEG was assessed by the SPR angle shift. To increase the amount of PEG, the process of PEG introduction was repeated several times. Namely, after introduction of PEG on the sensor surface as stated above, the acetal-PEG-SH solution was injected again, followed by washing with 0.05 M NaOH in the same way as mentioned above. PEGylated surfaces prepared by one, two, and four repetitive introductions were denoted as PEG5k-(1), PEG5k(2), and PEG5k(4) surfaces, respectively. In a way similar to the above-mentioned repeated process, a successive PEGylation with longer and then shorter PEG was carried out. On the surface with the preconstructed longer PEG brushes (PEG5k(1) surface), a shorter PEG (PEG2k) as a filler was layered by repetitive introduction. PEG5k(1) surfaces with single and triple treatments with the filler PEG were denoted as PEG5k/2k(1/1) and PEG5k/2k(1/3) surfaces, respectively.

Nonspecific Protein Adsorption. Adsorption of BSA on the prepared PEGylated surfaces was monitored by SPR. A solution of 1 mg/mL BSA in 0.01 M HEPES buffer was allowed to flow onto these PEGylated surfaces for 10 min at a flow rate of 20 μL/min at 25 °C, following the injection of HEPES buffer for 3 min at the same rate. The magnitude of the SPR angle shift by this successive injection was measured and assessed as the amount of BSA adsorbed. As a control, BSA adsorption on a conventionally used CM5 chip was examined.

Introducing Biotin to the α-Acetal-ω-mercapto-PEG Tethered Chain. Biotinylation of the free end group of the tethered PEG was conducted by the acid hydrolysis of the acetal end group, followed by a reaction with biocytin hydrazide. This treatment was carried out before the backfilling PEG unless stated otherwise. A solution of 0.01 M HCl was allowed to flow onto the gold sensor chip modified with acetal-PEG at 5 μL/min for 60 min at 37 °C to convert the acetal group to an aldehyde group. Biocytin hydrazide (0.7 mg/mL) in sodium phosphate buffer (pH 7.4, 0.05 M) was then injected at 10 μL/min at 37 °C. In this way, the biotin moiety was introduced at the distal end of PEG through Schiff base formation. The amount of introduced biotin was assessed by the SPR angle shift. The surface with biotinylated PEG was denoted as PEG-b; for example, the biotinylated PEG5k(1) surface was described as PEG5k−b(1).

Recognition of Streptavidin on the Biotinylated PEG Surface. PEG5k(4) surface was constructed by four repetitive introductions of PEG5k as mentioned above. After the construction

(23) Mori, Y.; Nagaoka, S.; Takiuchi, H.; Kikuchi, T.; Noguchi, N.; Tanzawa, H.; Noishiki, Y. *Trans. Am. Soc. Artif. Intern. Organs* **1982**, *28*, 459−463.
(24) Bergdtröm, K.; Österberg, E.; Holmberg, K.; Hoffman, A. S.; Schuman, T. P.; Kozlowski, A.; Harris, J. M. *J. Biomater. Sci. Polym. Ed.* **1994**, *6*, 123−132.
(25) Harris, J. M., Ed. *Poly(ethylene glycol) Chemistry: Biotechnical and Biomedical Applications*; Plenum Press: New York, 1992.
(26) Glass, J. E., Ed. *Hydrophilic Polymers: Performance with Environmental Acceptance*; American Chemistry Society: Washington, DC, 1996.
(27) Lin, Y. S.; Hlady, V.; Golander, C. G. *Colloids Surf., B* **1994**, *3*, 49−62.
(28) Jeon, S. I.; Andrade, J. D.; de Gennes, P. G. *J. Colloid Interface Sci.* **1991**, *142*, 159−166.
(29) Antonsen, K. P.; Hoffman, A. S. *In Poly(ethylene glycol) Chemistry: Biotechnical and Biomedical Applications*; Harris, J. M., Ed.; Plenum Press: New York, 1992; pp 15−28.
(30) Abbott, N. L.; Blankschtein, D.; Hatton, T. A. *Macromolecules* **1992**, *25*, 5192−5200.
(31) Otsuka, H.; Nagasaki, Y.; Kataoka, K. *Biomacromolecules* **2000**, *1*, 39−48.
(32) Nagasaki, Y.; Kutsuna, T.; Iijima, M.; Kato, M.; Kataoka, K.; Kodama, Y. *Bioconjugate Chem.* **1995**, *6*, 231−233.
(33) Nagasaki, Y.; Ogawa, R.; Yamamoto, S.; Kato, M.; Kataoka, K. *Macromolecules* **1997**, *30*, 6489−6493.
(34) Akiyama, Y.; Otsuka, H.; Nagasaki, Y.; Kato, M.; Kataoka, K. *Bioconjugate Chem.* **2000**, *11*, 947−950.
(35) Otsuka, H.; Akiyama, Y.; Nagasaki, Y.; Kataoka, K. *J. Am. Chem. Soc.* **2000**, *123*, 8226−8230.

of the PEG5k(4) surface, the biotinylation was carried out and denoted as PEG5k-b(4). On the PEGylated gold sensor chips with or without the biotin end group, viz., PEG5k-b(4) or PEG5k(4) surfaces, a solution of 6 μg/mL streptavidin in 0.01 M HEPES buffer was injected at a flow rate of 20 μL/min for 10 min at 25 °C, followed by the injection of HEPES buffer for 3 min at the same rate. The magnitude of the SPR angle shift by this successive injection was measured to assess the amount of streptavidin bound to each surface. An untreated gold surface was used as a control.

In the same way as mentioned above, the SPR angle shift for streptavidin was monitored on the PEG2k-b-tethered chain surfaces without and with a longer filler PEG5k and on the PEG5k-b-tethered chain surfaces without and with a shorter filler PEG2k.

SPR Sensing of Streptavidin from a Mixed Protein Solution. On two kinds of PEGylated gold sensor chips, PEG5k-b/2k(1/3) and PEG5k-b(1) surfaces, a mixed solution of 0.1 μg/mL streptavidin and 1 mg/mL BSA, a 10^4 excess relative to the former, was injected at a flow rate of 20 μL/min for 10 min at 25 °C, followed by the injection of HEPES buffer for 3 min at the same rate. The magnitude of the SPR angle shift by this successive injection was measured to assess protein adsorption. A 0.1 μg/mL streptavidin solution was used as a control.

Influence to SPR sensing of streptavidin by the length of the filler PEG. To assess the effect of the chain length of the filler layer, two types of mixed tethered chains were prepared, viz., biotin molecules at the free chain end of PEG-5k and −2k, respectively. In the case of the mixed PEG tethered chains (5k/2k) having the biotin molecule at PEG5k, after the modification of PEG5k (SPR angle shift of 0.18°, which was controlled by the SPR flow time of the PEG5k solution), biocytin hydrazide was conjugated in the same manner as stated above. The amount of modified biotin was also controlled by the SPR flow time (0.015°). To the prepared surface, PEG2K was modified (PEG5k-b/2k). PEG2k-b/5k was also prepared in the same manner.

RESULTS AND DISCUSSION

Two lots of α-acetal-ω-mercapto-PEG with different molecular weights were synthesized according to our established method.[34,25] The molecular weight and the molecular weight distribution of the synthesized PEGs, denoted as PEG5k and PEG2k, were 4990 and 1.04 and 1920 and 1.03, respectively. PEGylation of the SPR gold sensor surface was done in sodium phosphate buffer containing 1 M NaCl. The use of the buffer with high ionic strength caused an increase in the amount of tethered PEG, due to the reduced solubility of PEG in the buffer solution.[36] From the result of SPR analysis, the use of the buffer with 1 M NaCl induced an increase of the SPR angle shift for tethered PEG by ~40% in comparison to that without NaCl (data not shown).

Nonspecific protein adsorption on the PEGylated surface was evaluated using BSA as a model protein. A bare gold and a commercial carboxymethylated dextran surface (CM5) were used as a control. The SPR angle shift due to the nonspecific adsorption of BSA was (802 ± 176) × 10^{-4}° and (58.9 ± 12.3) × 10^{-4}° for a bare gold and the CM5 surfaces, respectively, when 1 mg/mL BSA solution flowed for 10 min. The amount of adsorbed BSA was gradually increased until 30 min. On the contrary, the PEG5k surface showed very low BSA adsorption ((24.1 ± 4.3) × 10^{-4}°) under the same conditions. It should be noted that no increase in the adsorbed amount was observed after 10 min. Thus, evaluation of the protein interaction on the PEGylated surface was carried out for 10 min. An SPR angle shift of 1.0° on the CM surface was reported to correspond to ~1 μg/cm^2.[4,14] If this relation is applicable for the PEGylated surface, the amount of the adsorbed BSA on the bare gold, CM, and PEG5k surfaces were estimated as 80.2 ± 17.6, 5.9 ± 1.2, and 2.4 ± 0.4 ng/cm^2, respectively. It should be noted that the thickness of the tethered PEG layer is estimated to be below ~10 nm,[37,38] whereas the dextran[3] gel has ~100-nm thickness. It is well known that the sensitivity of SPR is in an inverse proportional relation to the distance from the gold surface.[14,37,39] Thus, the PEG5k tethered chain surface is likely to have the more remarkable nonfouling character than the conventional CM hydrogel, even though the former has the shielding layer ~1/10 thinner than that of the latter. Though PEG5k appreciably reduced the nonspecific BSA adsorption, there was still a slight, but definite, adsorption of BSA, which may hamper the specific sensing ability in actual use. To further decrease the nonspecific adsorption of BSA on the PEG layer, an increase in PEG density on the surface may be absolutely imperative. Repeated introduction of the PEG chain to the preconstructed PEG brush surface was then carried out to increase the surface density of PEG. After a first treatment with PEG5k, the sensor surface was washed with the buffer and a solution of 0.05 M NaOH in order to remove noncovalently adsorbed PEG. The sensor chip was then treated with a solution of PEG5k again. This cycle of adsorption/rinsing of PEG5k was repeated several times. By rinsing, a reduction in the SPR angle shift was observed on the surface with PEG5k, indicating that noncovalently adsorbed PEG was removed. Retreatment with PEG5k caused a reincrease in SPR angle shift.[40] Eventually, the total SPR angle shift was amplified by increasing the treatment cycles to four, indicating that repetitive treatment with PEG5k was effective in increasing the density of PEG. According to the simplified calculation for estimating the effective adlayer density on the gold surface from the measured SPR response,[37-38] the average PEG adlayer density was calculated, and the results were shown in Table 1. Nonspecific adsorption of BSA on the PEG5k layer with varying numbers of treatment cycles was evaluated as the amount of adsorption (ng/cm^2) from the measured SPR angle shift, and the results are also listed in Table 1. With increasing treatment cycles, the nonspecific adsorption of BSA was dramatically reduced. Thus, the repeated treatment was indeed effective in preventing nonspecific protein adsorption. Notably, this trend became even more significant by the additional treatment of the PEG5k(1) surface with shorter PEG (PEG2k) as seen in Table 1. Our hypothesis was to increase the surface brush density by PEG2k, retaining the PEG5k brush surface character. After a first treatment with PEG5k, the surface was treated with PEG2k by a repeated adsorption/rinse procedure as stated above. The density of the PEG layer from the total SPR angle shift induced by this adsorption/rinse treatment with PEG5k and -2k is also summarized in Table 1. Obviously, successive

(36) Emoto, K.; Harris, J. M.; Alstine, M. V. *Anal. Chem.* **1996**, *68*, 3751−3757.
(37) Jung, L. S.; Campbell, C. T.; Chinowsky, T. M.; Mar, M. N.; Yee, S. S. *Langmuir* **1998**, *14*, 5636−5648.
(38) Lu, H. B.; Campbell, C. T.; Gastner, D. G. *Langmuir* **2000**, *16*, 1771−171.
(39) Liedberg, B.; Lundström, I.; Stenberg, E. *Sens. Actuators, B* **1993**, *11*, 63−72.
(40) Refer to Supporting Information.

Table 1. Relation between the Adsorbed Mass of PEG and BSA on the Gold Surface

surface[a]	SPR response (deg)		density (ng/cm^2)	
	PEG	BSA[b]	PEG[c]	BSA[d]
bare gold		$802 \pm 176 \times 10^{-4}$		80.2 ± 17.6
PEG5k(1)	0.150 ± 0.015	$24.1 \pm 4.3 \times 10^{-4}$	230 ± 23	2.41 ± 0.43
PEG5k(2)	0.194 ± 0.027	$17.0 \pm 3.2 \times 10^{-4}$	298 ± 42	1.70 ± 0.32
PEG5k(4)	0.239 ± 0.022	$7.6 \pm 2.5 \times 10^{-4}$	366 ± 34	0.76 ± 0.25
PEG5k/2k(1/1)	0.219 ± 0.018	$4.0 \pm 1.6 \times 10^{-4}$	335 ± 27	0.40 ± 0.16
PEG5k/2k(1/3)	0.298 ± 0.025	$1.1 \pm 1.1 \times 10^{-4}$	456 ± 39	0.11 ± 0.11

[a] PEGylation of a gold SPR sensor surface by repetitive PEG modification: PEG5k(1), PEG5k(2), and PEG5k(4) surfaces are prepared by the modification of α-acetal-ω-mercapto-PEG having the M_w of 5 kDa, where the number in parentheses denotes the number of modification cycles; PEG5k/2k(1/1) and PEG5k/2k(1/3) surfaces are prepared, respectively, by single and triple modifications of the PEG5k(1) surface with α-acetal-ω-mercapto-PEG having M_w of 2 kDa. [b] The SPR angle shift for BSA adsorption by using 1 mg/mL BSA solution at a flow rate 20 μL/min for 10 min at 25 °C. [c] PEG adlayer density is estimated from the total SPR response for the PEG modification.[37,38] [d] The adsorbed mass of BSA is calculated from SPR response for adsorbed BSA.[4,14]

surface treatment with PEG5k and -2k induced a more significant SPR angle shift compared to the repeated treatment with only PEG5k, indicating the former to have a higher PEG surface density than the latter. Furthermore, as can be seen in Table 1, the PEG5k/2k(1/1) surface showed remarkably lower nonspecific adsorption of BSA than PEG5k(2). Notably, by triple treatment with PEG2k of the PEG5k(1) surface (PEG5k/2k(1/3)), nonspecific BSA adsorption was almost complete suppressed, 1.1×10^{-4}°, namely, ~0.1 ng/cm^2. On the basis of these results, it was concluded that an essentially nonfouling surface[40] was constructed by the successive surface treatment with PEG having a molecular weight of 5000 (PEG5k) and a shorter PEG (PEG2k) that formed the underbushed PEG layer.

The α-acetal group of the PEG in aqueous solution was quantitatively converted into an aldehyde group by acid treatment such as 0.01 M HCl. The conversion reaction on the surface tethered chain end was confirmed by an ESR measurement after an installation of ESR probe (4-amino-TEMPO).[31] Due to the high reactivity of aldehyde groups toward primary amino groups,[31,35] various ligands including proteins and peptides can be covalently conjugated to the distal end of the tethered PEG chains. In this study, biotin, a molecule showing specific affinity for streptavidin, was bound to PEG as a model ligand molecule.

Biotin having a hydrazide moiety (biocytin hydrazide) was installed at the distal end of the PEG tethered chain on a PEG5k-(4) surface constructed using four repeated treatments with PEG5k. The biotin-conjugated PEG5k(4) surface was denoted as the PEG5k-b(4) surface. SPR sensing of streptavidin (6 μg/mL) binding to the PEG5k-b(4) chip was then examined. A bare gold chip and a PEG5k(4) chip without biotin were used as controls. Obviously, there was essentially no adsorption of streptavidin on the PEG5k(4) chip as shown in Figure 1. This is in sharp contrast to the bare gold surface showing a significantly high nonspecific adsorption of streptavidin. Highly specific recognition of streptavidin by the system of PEG5k-b(4) was confirmed through the significant shift in the SPR angle with the injection of streptavidin solution into the SPR flow channel.

To assess the specific sensing of streptavidin in a mixed solution of protein by a biotinylated PEG5k surface, the BSA solution (1 mg/mL) containing 0.1 μg/mL streptavidin was injected into the SPR system equipped with the PEG5k-b(1) or PEG5k-b/2k(1/3) sensor chip. The results are summarized in Table 2. The PEG5k-b(1) system showed a higher SPR signal upon

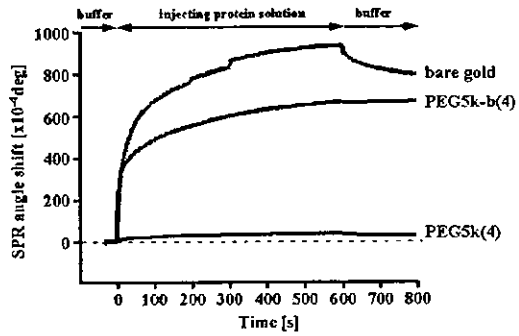

Figure 1. SPR sensorgrams for the binding of streptavidin to the bare gold, PEG5k-b(4) and PEG5k(4) surfaces using 6 μg/mL streptavidin solution at a flow rate of 20 μL/min for 10 min at 25 °C. At time zero, the flowing solution is switched from HEPES buffer to the streptavidin solution and the alternation of their solutions at 600 s (10 min). PEG5k(4) surface has acetal groups at the end of PEG5k tethered chain surface, on the other hand, PEG5k-b(4) surface has biotin moieties. On the PEG5k with aldehyde groups tethered chain surface, biocytin hydrazide was introduced, and SPR angle shift for biotinylation was 0.030 ± 0.009°. This surface was denoted as a PEG5k-b(4) surface.

Table 2. Effect of a Filler PEG Layer on the Specific Recognition of Streptavidin

surface[a]	adsorbed mass (ng/cm^2)	
	streptavidin/BSA mixture[b]	streptavidin[c]
PEG5k-b(1)	531 ± 52	455 ± 40
PEG5k-b/2k(1/3)	449 ± 30	439 ± 27

[a] The mass of biocytin hydrazide binding to the end of the PEG5k chain is estimated at 20±3 ng/cm^2 from SPR angle shift.[4,14] (n = 4, ±SEM). [b] The adsorbed mass of protein from a mixture of 0.1 μg/mL streptavidin and 1.0 mg/mL BSA is calculated from the SPR angle shift.[4,14]. [c] The adsorbed mass of protein from 0.1 μg/mL streptavidin is calculated from theSPR angle shift.[4,14]. The SPR angle shifts on the biotinylated PEG surfaces by flow of the protein solution at a flow rate 20 μL/min for 10 min at 25 °C.

the injection of the streptavidin/BSA mixed solution compared to that obtained for the pure streptavidin solution. This increased response by the mixed protein solution is the contribution from the nonspecific adsorption of BSA. Worth noting is that coexisting BSA has almost no effect on the SPR signal in the case of the

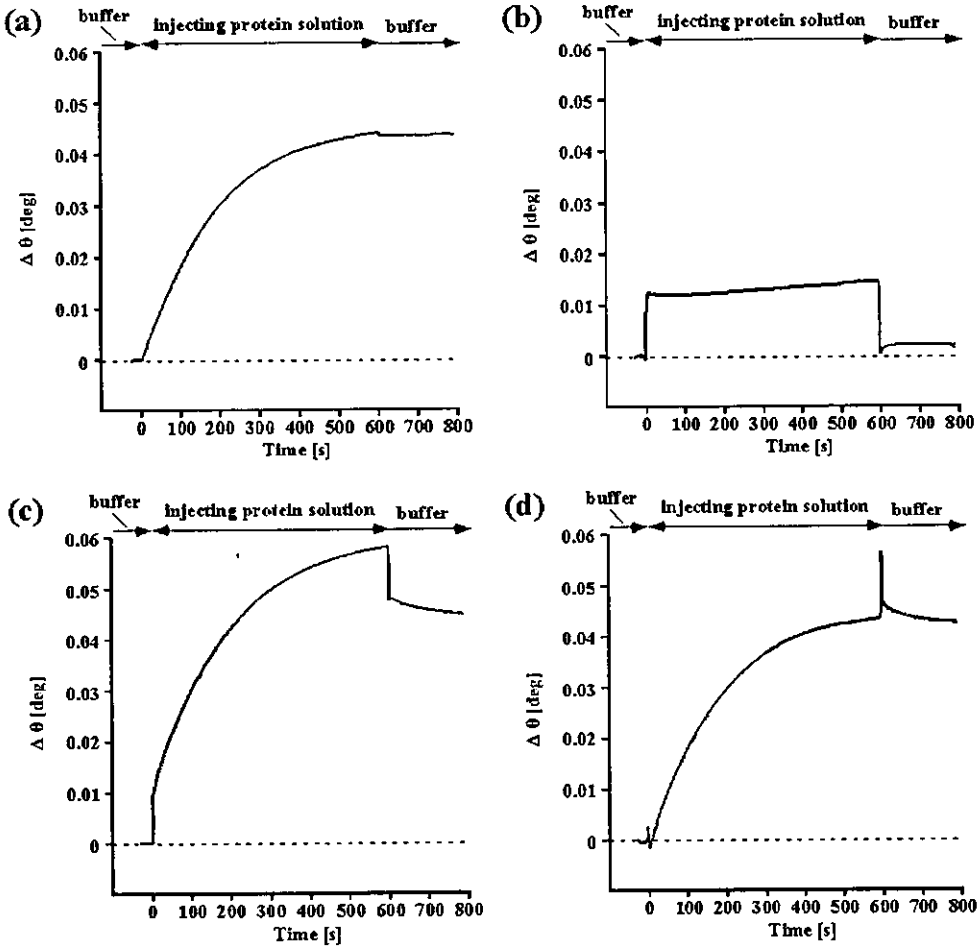

Figure 2. SPR sensorgrams of protein adsorption on the PEG5k-b/2k(1/3) surface from (a) 0.1 μg/mL streptavidin, (b) 1.0 mg/mL BSA, and (c) the mixture of 0.1 μg/mL streptavidin and 1 mg/mL BSA at a flow rate of 20 μL/min for 10 min at 25 °C. The sensorgram calculated by subtracting the SPR sensorgram of 1 mg/mL BSA from that of the mixture is shown in (d). PEG5k-b/2k(1/3) surface is the PEG5k with biotin moieties tethered chains surface having the backfilling of PEG2k. The mass of biocytin hydrazide binding at the end of PEG5k chain is estimated 20 ± 3 ng/cm^2 from the SPR angle.[4,14] (n = 3, ±SEM)

mixed brush surface of PEG5k-b/2k(1/3). The nonspecific character was also confirmed by the SPR sensorgrams shown in Figure 2. Panels a and b of Figure 2 show the sensorgrams of 0.1 μg/mL streptavidin and 1 mg/mL BSA, respectively. Due to the bulk effect, the angle shift of ~0.01° was observed when 1 mg/mL BSA solution was flowing. When the mixture of 0.1 μg/mL streptavidin and 1 mg/mL BSA flowed, the sensorgram was exactly the same as the streptavidin sensorgram along with the bulk effect due to the 1 mg/mL BSA solution. Obviously, the subtracted SPR sensorgram (Figure 2d = 2c − 2b) completely overlapped with that obtained in the presence of streptavidin (Figure 2a), indicating that excess BSA had negligible effect on sensing of streptavidin. It was confirmed again that the mixed PEG brush surface showed an appreciable nonfouling character. The short underbrushed layer of PEG2k contributed to minimizing the nonspecific adsorption of BSA.

To obtain further information on the sensing of biotin at the free end of the PEG tethered chain, two models of PEGylated surfaces were prepared. One was a PEGylated surface possessing a short PEG chain (2k) with biotin and a long PEG chain (5k) without biotin, denoted PEG2k-b/5k. The other was an alternative combination, which means that the sensor chip possessed a short PEG chain (2k) without biotin and a long PEG chain (5k) with biotin, denoted PEG5k-b/2k. Those are schematically illustrated in Figure 3. To assess the effect of PEG chains without a ligand end group, the amount of first modification of PEG was controlled in the range of angle shift of 0.13−0.18° to introduce a certain amount of the second PEG. Construction of these model surfaces was monitored by the SPR angle shift, and the data are summarized in Table 3. PEG2k-b and PEG5k-b were used as controls of this study. The SPR sensorgrams for streptavidin binding on these model surfaces are seen in Figure 3. Compared to the PEG2k-b surface, the introduction of PEG5k among the PEG2k-b brushes appreciably reduced the SPR response to streptavidin (Figure 3a). These results indicated that a longer PEG chain hindered the specific interaction of steptavidin with biotin at the distal end of the shorter PEG chain due to the excluded volume effect of the longer PEG chain; viz. the protein could hardly access the free end of the shorter chain because of the existing longer PEG chain. Worth noting is that, by a treatment with PEG2k of the PEG5k-b surfaces, the SPR response to streptavidin was definitely increased (Figure 3b). Further worth mentioning is that